



## Biopolymers as bone substitutes: a review

Cite this: DOI: 10.1039/c9bm00664h Anastasiia Kashirina, <sup>a</sup> Yongtao Yao,<sup>b</sup> Yanju Liu<sup>a</sup> and Jinsong Leng <sup>\*b</sup>

Received 26th April 2019,  
Accepted 10th July 2019  
DOI: 10.1039/c9bm00664h  
rsc.li/biomaterials-science

Human bones have unique structures and characteristics, and replacing a natural bone in the case of bone fracture or bone diseases is a very complicated problem. The main goal of this paper was to summarize the recent research on polymer materials as bone substitutes and for bone repair. Bone treatment methods, bone substitute materials as well as their advantages and drawbacks, and manufacturing methods were reviewed. Biopolymers are the most promising materials in the field of artificial bones and using biopolymers with the shape memory effect can improve the integration of an artificial bone into the human body by better mimicking the structure and properties of natural bones, decreasing the invasiveness of surgical procedures by producing deployable implants. It has been shown that the application of the rapid prototyping technology for artificial bones allows the customization of bone substitutes for a patient and the creation of artificial bones with a complex structure.

## 1. Introduction

### 1.1 The problem of bone fractures

Bones support the bodies of humans throughout their lives. Since ancient times, people have experienced breaking of bones because of accidents, resulting in serious injuries,

extreme sports, traffic accidents, aging and bone diseases. Furthermore, due to low bone density and osteoporosis, bones become weak and can break easily; osteogenesis imperfecta makes bones brittle; Paget's disease makes them weak; cancer, infections and other bone diseases can be caused by insufficient nutrition, genetics, or bone growth or rebuilding problems.<sup>1</sup> Pediatric fractures are frequently treated conservatively and only 8% cases require internal fixation; for the older category ( $\geq 16$  years of age), 56% patients require internal fixation.<sup>2</sup> A simple thing such as falling can change older adults' lives. Thousands of older people fall every year. For older people, a bone fracture can be the start of serious problems,

<sup>a</sup>Department of Astronautical Science and Mechanics, Harbin Institute of Technology, PO Box 301, No. 92 West Dazhi Street, Harbin 150001, China

<sup>b</sup>National Key Laboratory of Science and Technology on Advanced Composites in Special Environments, Harbin Institute of Technology, No. 2 Yikuang Street, Harbin 150080, China. E-mail: lengjs@hit.edu.cn



Anastasiia Kashirina

Anastasiia Kashirina obtained her master's degree at the Saint-Petersburg State Polytechnic University (Russia) in 2011. After graduation, she worked at the Central Research Institute of Structural Materials "Prometey" (Saint-Petersburg) as an engineer in the Department of Functional Materials, Nanomaterials and Coatings. Currently, she is a Ph. D. student at the Harbin Institute of Technology (HIT), School of Astronautics. She is

majoring in Materials Science; her research interests include biopolymers for inner-body applications, polymers with shape memory effect, and deployable implants.



Yongtao Yao

Prof. Yongtao Yao is an assistant professor at the Center for Composite Materials and Structures at the Harbin Institute of Technology. He obtained his doctorate from the Institute for Materials Research and Innovation at the University of Bolton in 2010. Then, he was engaged at the Center for Composite Materials and Structures at HIT as an assistant research fellow. His research field mainly focuses on the inves-

tigation of nanocomposite and auxetic materials and their applications. Till now, he has authored and co-authored more than 60 scientific papers.

such as hospitalization, injury, or even disability.<sup>3</sup> According to the World Health Organization data, the number of aged people is quickly increasing.<sup>4</sup> The amount of people over 60 years old is expected to be 2 billion in 2050 compared to 900 million in 2015 (increasing from 12% to 22% of the total population). Thus, serious fractures and bone diseases are very important problems, especially among the elderly.<sup>5</sup> A fracture treatment for the elderly and people from other high-risk groups (car drivers, factory workers, sportsmen, *etc.*) is required.

## 1.2 Bone fracture treatment methods

Bones unlike many other tissue types can regenerate. In view of this, bone grafting is possible for bone fracture treatment. Nowadays, bone grafting is the most frequently used method of bone fracture treatment.<sup>6,7</sup> Four types of bone grafts exist:

1. The use of autologous (or autogenous) bone grafts is the gold standard of bone grafting. It involves using the bone taken from the same person who receives the graft. A bone graft can be harvested from non-essential bones: the iliac crest, usually in dental and maxillo-facial surgery, the mandibular symphysis (chin area), or anterior mandibular ramus (the coronoid process). Autogenous bone grafts are the most commonly used grafts because of the lower risk of bone graft failure as the graft is derived from the individual's own body. The disadvantages of autologous bone grafts include the need for an additional incision, feeling pain after surgery for a long time and the possibility of increased blood loss during surgery. Even using the patient's own bone cannot guarantee 100% success.

2. An allograft is a bone derived from a cadaver or an individual who has donated his/her bones for the treatment of other people. In this method, the failure rate is high compared to using the patient's own bone and finding a suitable bone is a very difficult task.<sup>8,9</sup>

3. Xenografts are bone substitutes removed from a donor other than humans and they are grafted into a human body (bovine and porcine bones, natural corals).<sup>10</sup> Xenografts are commonly applied as a calcified matrix. Both allografts and xenografts exclude donor site complications, but some biological properties (osteogenic and osteoinductive) can be reduced.<sup>11</sup> Moreover, a bovine xenograft may not be the most relevant choice for foot and ankle surgery.

4. Artificial bones: Commonly studied artificial bone biomaterials are titanium alloys,<sup>12,13</sup> zirconia,<sup>14</sup> steel,<sup>15,16</sup> bioceramics (including bioglasses)<sup>17–19</sup> and polymer materials for tissue engineering.

Autogenous bones have optimal biological properties, but the donor's morbidity (pain, blood tumor, infection, and fracture) and limited availability are challenging factors. On the contrary, allogeneic (genetically different) and artificial grafts are expensive, may cause an inflammatory response and transmit diseases, can be difficult to produce, and have limited osteogenic or osteoconductive properties.<sup>20,21</sup>

Some research papers have reported that several metal ions (from Ni-Ti, Co-Cr-Mo-Ni-Fe, stainless steel, Ti alloys, or pure Ti) are released into surrounding tissues because of a wide range of mechanisms including corrosion. Metal ion release is often considered as a cause of clinical failure or a dermic allergic reaction.<sup>22–24</sup> Metals have good mechanical



Yanju Liu

*Dr Yanju Liu is a professor at HIT. Her research interests are the design of shape memory polymers and composites, 4D printing, and mechanical behavior and structures. She has authored and co-authored more than 150 SCI papers and 70 invention patents and edited five book chapters. She is the Deputy Editor of the Journal "Smart Materials and Structures", the Director of the Intelligent Composite Material Professional*

*Committee of the Chinese Composite Society, and the Director of the Continental Association of the International Advanced Materials and Manufacturing Engineering Society. She has won the National Natural Science Prize, National Technological Invention Prize, and National Defense Technological Inventions Prize.*



Jinsong Leng

*Prof. Jinsong Leng is the Cheung Kong Chair Professor and Director of the Center for Smart Materials and Structures at HIT. His research covers sensors and actuators, stimulus-responsive polymers, multifunctional nanocomposites, active vibration control, structural health monitoring, and active deployable or morphing structures. He has served as the Vice President of the International Committee on Composite Materials (ICCM)*

*and the Chinese Society for Composite Materials (CSCM), the Chairman of the Asia-Pacific Committee on Smart and Nano Materials (APCSNM), and the Editor-in-Chief of the International Journal of Smart and Nano Materials. He is a World Fellow and an Executive Council Member of ICCM, Member of the Academia Europaea and the European Academy of Sciences and Arts, Fellow of the AAAS, the SPIE, Institute of Physics (IOP), Royal Aeronautical Society (RAeS), and Institute of Materials, Minerals, and Mining (IMMM) and Associate Fellow of AIAA.*

properties but in most cases, they do not interact with the body cells and are very strong compared to natural bones, which can lead to stress shielding, bone loss and bone relaxation.<sup>25–27</sup> Bioactive ceramics have a similar composition to that of natural bones and show excellent biocompatibility and bioactivity. However, their typical brittleness and low toughness limit their applications in bone repair.<sup>28</sup>

In comparison, biopolymers (including natural and synthetic polymer-based composites) are very promising biomaterials for fabricating medical products and bone substitutes due to good biocompatibility, adjustable chemical composition and biodegradation, and the ability to reorganize.<sup>29</sup>

The main goal of this paper was to present the recent research on polymer materials for bone implants and bone repair.

### 1.3 Requirements for bone substitute materials

In terms of such a complex biological and sensitive system as the human body, the requirements for tissue engineering materials are extremely challenging<sup>30</sup> and are detailed as follows:

1. Porosity: Bone-like porous structures provide nutrient movement, blood circulation, and passage of osteogenic cells and bioactive components, which in conjunction promote mineralization and blood vessel formation throughout the graft. The structure of bones is shown in Fig. 1.<sup>31</sup>

2. Bone substitute surface roughness: The surface roughness is an important factor not only in the initial adhesion, but also in the activity and differentiation of osteoblasts.<sup>32</sup>

3. Biocompatibility: This involves the integration of a bone implant into natural bone tissues or simply into the human body to intensify the tissue repair process.

4. Biodegradability: This involves an adjustable rate of degradation over time while bone tissue regeneration occurs.

5. Mechanical properties: Mechanical properties similar to those of natural bones are necessary for successful bone grafting. The scaffold must provide support during the bone ingrowth process until the new bone has enough coherence to support itself.<sup>33</sup>

6. Positive interactions between the bone substitute material and body cells are necessary for cell functions (adhesion, proliferation, differentiation, and gene expression).<sup>34,35</sup>

7. The production time cannot be very long because a patient cannot wait for one or two weeks.

So far, a material that can meet all these requirements for bone substitutes does not exist. However, with the development of modern technology, material properties are getting increasingly closer to those of natural bones. This review shows the recent progress in material science for bone substitutes and emphasizes on creating scaffolds with a natural bone-like structure and mechanical properties.

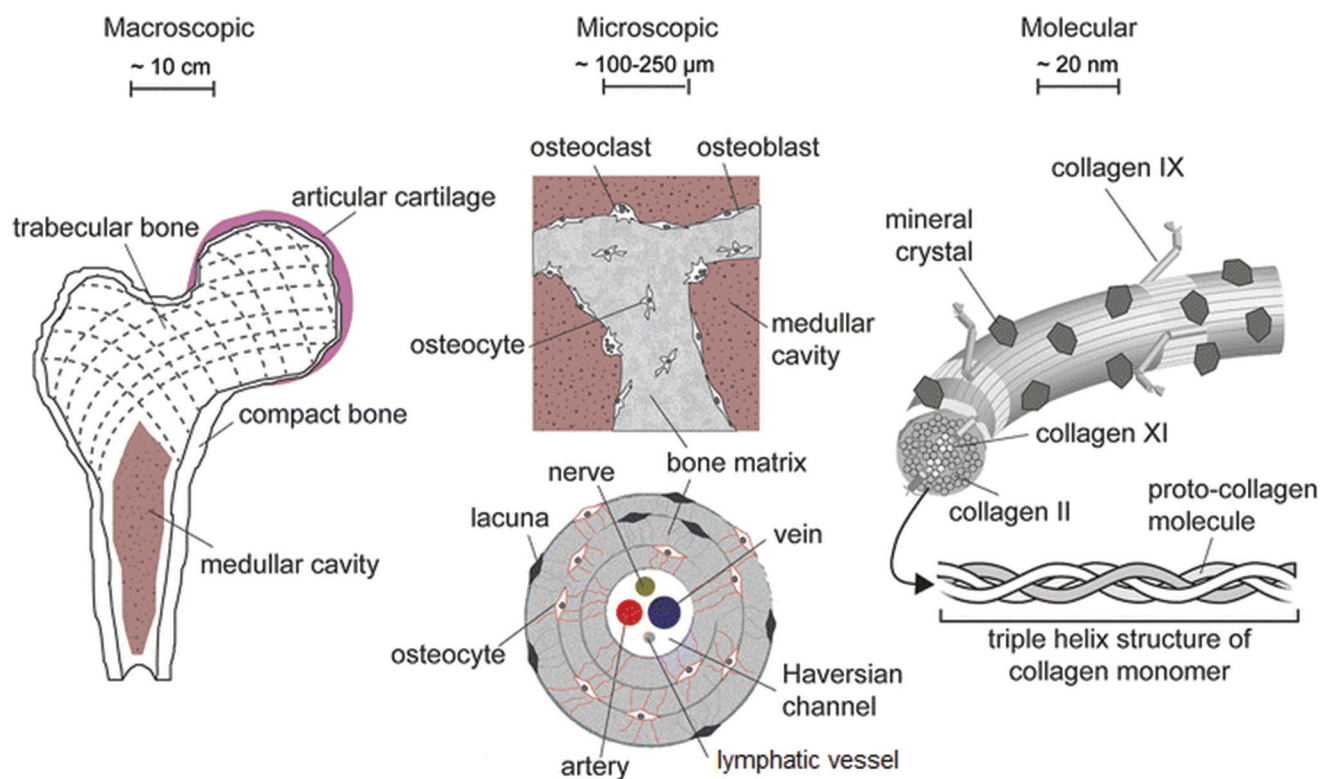


**Fig. 1** Structural organization of bones from macroscopic to molecular levels. Reproduced with permission from ref. 31, copyright 2018, Springer Nature, distributed under the Creative Commons CC BY license.

## 2. Review of polymer bone materials in 2015–2019

### 2.1 Natural biopolymers

**Collagen materials.** Saska *et al.* fabricated nanocomposites based on bacterial cellulose (BC), collagen (COL), apatite (Ap, *in situ* precipitation was used to incorporate Ap into the BC-COL matrix), and osteogenic growth peptide (OGP) or its C-terminal pentapeptide [OGP(10–14)] incorporated into the (BC-COL)-Ap composite by absorption for bone regeneration.<sup>36</sup> All composites did not show cytotoxicity, genotoxicity and mutagenicity; they stimulated cell growth at an earlier time than the pure bacterial cellulose sample. The tensile strengths of (BC-COL)-Ap before ( $57.7 \pm 1.8$  MPa) and after gamma radiation sterilization ( $45.0 \pm 4.0$  MPa) were reported. Despite the decreased tensile strength of the (BC-COL)-Ap composites compared to that of BC, (BC-COL)-Ap-OGP or OGP(10–14) may be considered as potential materials for bone repair due to their good biocompatibility.

One of the key mechanisms of bone substitutes is providing a “template” for new bone ingrowth. Ren *et al.* investigated mineralized collagen/glycosaminoglycan (MC-GAG) scaffolds. Animal (rabbit) experiments showed that the MC-GAG implants had better ability to support the bone repair of cranial defects than non-mineralized collagen/glycosaminoglycan scaffolds.<sup>37</sup> Although the MC-GAG scaffolds exhibited increased healing ability even without the addition of *ex vivo* cultures with bone marrow-derived mesenchymal stem cells (BMSCs) or an exogenous growth factor, the authors considered that the scaffold strength was still less than that of a native rabbit bone and the stiffness was 50–80% of that of a natural bone. Zhang *et al.* fabricated cross-linked sponge-like collagen/hydroxyapatite composites by lyophilization, followed by a dehydrothermal process.<sup>38</sup> The spectra of the composites were similar to that of a rabbit bone, and animal experiments on rabbits showed an induced bone repair effect at defects with sizes exceeding the critical size for self-recovery. Mechanical tests revealed tensile strengths in the range of about 0.1–0.38 MPa and Young moduli in the range of 2900–8700 MPa; the sample with a collagen : HA ratio of 5 : 5 was very soft. The decomposition time in a Tris-buffered saline solution at 37 °C was in the range from 180 to 5640 min. Thus, it can be suggested that MC-GAG and COL : HA composites may be used in non-bearing applications to induce the bone repair process.

**Chitosan composites.** Chitosan (CS) is a linear polysaccharide commonly produced by the partial deacetylation of chitin.<sup>39</sup> CS has widespread use in bone tissue engineering due to its osteoconductivity for enhancing bone formation, good biodegradability, remarkable antibacterial activity, and excellent biocompatibility.<sup>40</sup> The composites of chitosan and hydroxyapatite were intensively tested, and their compressive strength could reach 119.86 MPa; however, an aquatic environment can significantly decrease the mechanical properties of a chitosan/hydroxyapatite composite material.<sup>41</sup>

Chen *et al.* prepared chitosan-silk sericin/hydroxyapatite (CS-SS/HA) composites using *in situ* precipitation.<sup>39</sup> The mechanical properties of the composites with organic components less than 50% were not sufficient; the best combination of elastic modulus and compressive strength was shown by the composites with 60 and 70% organic parts due to the brittleness of HA. The CS-SS/HA composites could promote osteoblast attachment and proliferation during experiments with the culturing of osteoblast cells on the samples.

Chitosan/nanohydroxyapatite/zoledronic acid scaffolds were prepared using the *in situ* precipitation method.<sup>42</sup> These scaffolds revealed excellent tumor inhibition properties, remarkable antibacterial activity and good osteoinductivity. Although the mechanical properties were not measured in this study,<sup>42</sup> porous CS/nHA/Zol is a promising biomaterial in bone tumor therapy and bone defect repair.

Wu *et al.* described one more problem, *i.e.*, the factor that limits the use of chitosan materials: degradation time.<sup>43</sup> It was emphasized that the degradation time of many biodegradable natural polymers, such as collagen, hyaluronic acid and chitosan, is still not long enough for the clinician-suggested period of 4–6 months. In this study, chitosan nanofiber membranes were obtained by electrospinning and then, the surface of the nanofibers was modified by butyrylation. The modification process prolonged the degradation time of the obtained chitosan membranes; thus, the modification of material surfaces may be useful for creating a chitosan-based bone repair material.

Elkholy *et al.* developed  $\beta$ -chitosan/nano-hydroxyapatite composites.<sup>44</sup> The optimum mechanical properties were obtained from the composites with 30 wt%  $\beta$ -chitosan (the compressive strength was 13.05 MPa). The animal experiments revealed enhanced bone regeneration and blood vessel incorporation. The total weight loss during experiments in citric acid and liquid ionomer glass cement solutions at room temperature could be reached at 8 weeks; thus, the composite material is very promising as a solid-shaped implant for relatively healthy patients without bone diseases and for non-critical size defects.

**Silk materials.** One of the most explored natural polymers for bone regeneration is silk.<sup>45</sup> It is a natural protein fiber produced by insect larvae to form cocoons (mulberry silkworm *Bombyx mori* larvae are the best known larvae to obtain silk cocoons).<sup>46</sup> Spider silk is light and has outstanding mechanical properties, but its use has been restricted due to its limited availability.<sup>45</sup> As Meinel *et al.*<sup>47</sup> reported, the use of silk materials may trigger an antigenic reaction.<sup>45</sup> However, creating composite materials with silk and applying cutting-edge technologies can help overcome this drawback.

The silkworm cocoon mainly consists of two proteins: silk sericin (SS) and silk fibroin (SF). Pure SS is not applied due to low mechanical properties, but the mitogenic ability of SS makes it beneficial for bone regeneration (to stimulate the formation of bone-like hydroxyapatite). Thus, the use of SS-based composites has to be considered.<sup>48</sup> In addition to composites

with chitosan and hydroxyapatite,<sup>39</sup> silk sericin can be used for biomimetic mineralization and regenerative medicine in the form of microcapsules. Mineralized sericin microcapsules with a hydroxyapatite shell on the surface showed good cytocompatibility and may be useful in drug delivery.<sup>49</sup>

In the case of silk fibroin materials, silk fibroin films and ultrathin films can approach the range of the mechanical strength of a natural bone: Young's modulus can reach 6–8 GPa with the ultimate strength of 100 MPa for nonporous films; however, silk films are still brittle and their breaking strain is in the range of 0.5–5.5%.<sup>50</sup> Researchers have attempted to overcome the lack of mechanical strength by creating composite materials.<sup>51</sup>

Bhattacharjee *et al.* reinforced nonmulberry tasar silk obtained from *Antheraea mylitta* with polyvinyl alcohol.<sup>52</sup> The electrospun nanofibers were 177–193 nm in diameter. The elongation at break was in the range of 14.5–23.6% (higher than that reported in the work of Koh *et al.*<sup>50</sup>), with the ultimate tensile strength of 4.87–12.55 MPa, but this value was still lower than the elongation at break for the silk composite prepared using a similar electrospinning process (recombinant silk fibroin produced with HFA-hydrate as a spinning solvent).<sup>53</sup>

In the study reported by Behera *et al.*, silk fibroin (obtained from the tropical nonmulberry tasar silkworm *Antheraea mylitta*) scaffolds were reinforced by fibroin-hydroxyapatite nanoparticles prepared by the chemical precipitation method.<sup>54</sup> The porous scaffolds (pore size 41–95  $\mu\text{m}$ ) had a Young's modulus of only 18.89 MPa; the scaffolds supported cell proliferation over time but without significant difference between the studied scaffolds and the commercial hydroxyapatite-reinforced fibroins in terms of cellular growth and proliferation.

In the other article by Bhattacharjee *et al.* to approach the requirements for bone substitute materials, poly( $\epsilon$ -caprolactone) was blended with silk fibroins (obtained from *Antheraea mylitta*) and nanofibrous mats were fabricated using the electrospinning method.<sup>55</sup> The ultimate strength and elongation at break values increased compared to the parameters of electrospun PCL (4.94–5.21 MPa and 19.32–29.1% for SF/PCL compared to 2.98 MPa and 14.1% for PCL, respectively).

Sahu *et al.* prepared nonmulberry *Antheraea mylitta* (Am, silkworms did not feed on mulberry leaves) silk fibroin scaffolds and *Bombyx mori* (Bm) silk fibroins.<sup>56</sup> Am fibroin scaffolds showed good bone regeneration in rat cranial defects and promoted the proliferation of osteoprogenitor cells compared to Bm. Both scaffolds were porous (60% for Bm and 66.66% for Am, with average pore sizes of 73 and 76  $\mu\text{m}$ , respectively), but their degradation rates had differences. Am scaffolds showed no signs of degradation up to 12 months, whereas Bm samples gradually degraded within 3 months. Also, the Bm samples did not support bone formation well. As the authors mentioned, very fast degradation can lead to mechanical graft failure and insufficient bone regeneration; thus, the Am scaffolds were suggested as better candidates for bone tissue repair materials mainly for non-bearing applications (cranial defects).

Ding *et al.* prepared demineralized bone matrix (DBM) powder/silk fibroin (SF) porous scaffolds using a solvent casting-salt leaching method.<sup>57</sup> The results of culturing rBMSCs on the samples showed that the composite with 20% DBM powder provided better cell proliferation and promoted cell attachment and growth. Using SF as a carrier for DBM powder helped overcome some drawbacks of DBM: difficulties in handling, migration from graft sites, and lack of stability after surgery. However, the mechanical properties showed that the most promising composite, *i.e.*, 20% DBM/SF had only  $1.12 \pm 0.16$  MPa compressive strength and  $2.41 \pm 0.51$  MPa compressive modulus; thus, there is an opportunity to use this material only for non-bearing repair.

$\beta$ -TCP ( $\beta$ -tricalcium phosphate) is a well-known reinforcing material for biocomposites due to its great osteoconductivity and biocompatibility. In the study by Park *et al.*,  $\beta$ -TCP was used in silk fibroin composites.<sup>58</sup> The addition of  $\beta$ -TCP particles to the silk scaffolds did not significantly increase the compressive strength of the composite materials (under 0.6 MPa for pristine SF scaffolds obtained by freeze-drying; 0.71–0.72 MPa for SF/ $\beta$ -TCP hybrid composites), and the addition of  $\beta$ -TCP did not influence the fibroblast growth *in vitro*. However, the SF/ $\beta$ -TCP samples showed faster bone regeneration in rat calvarial defects in comparison to the pure SF samples.

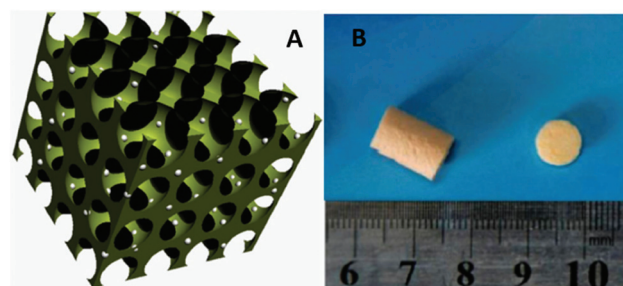
The highest mechanical properties within silk materials were found by Melke *et al.*<sup>51</sup> by reviewing the articles reported by Perez-Rigueiro *et al.*<sup>59,60</sup> The silk samples obtained by the forced reeling of *Bombyx mori* silkworms showed high mechanical strength (Table 1); however, forced silking is a time-consuming process and is not suitable for high-volume production.

Due to the low mechanical strength but great biocompatibility of silk materials, some attempts to use silk fibroin as a supporting material were made. Gentamicin-loaded silk fibroin (SFGM) was used to decrease the risk of postoperative infection and improve the biological functionality of porous Co–Cr–Mo scaffolds.<sup>61</sup> The Co–Cr–Mo metal scaffold was fabricated by selective laser melting and then, the electrophoretic deposition technique was applied to coat SFGM onto the Co–Cr–Mo alloy sample. With the average pore size of  $625.0 \pm 54.1$   $\mu\text{m}$  and the compressive properties, *i.e.*,  $\sim 75$  GPa for compressive strength and  $\sim 2.6$  GPa for elastic modulus compared to those ( $\sim 70$  GPa and  $\sim 2.4$  GPa, respectively) of non-coated Co–Cr–Mo, SFGM was suggested as a promising coating for biomaterials.

**Gelatin scaffolds.** Bioactive nanoparticles (BP)/gelatin scaffolds have been used to repair femoral defects in rabbits.<sup>62</sup> The bioactive nanoparticles (produced by surface modification on colloidal silica particles by  $\text{Ca}(\text{OH})_2$ )<sup>63</sup> have been proven to be promising additives for bone repair materials. The obtained scaffolds accelerated bone repair (the bone defects were almost filled with new bones 8 weeks after surgery compared to 12 weeks postoperation for rabbits without implants). The mechanical properties of the porous composite materials (Fig. 2) 8 weeks after surgery were higher but close to those of cancellous bones.

**Table 1** Mechanical properties of natural bone and some polymer materials for bone substitutes (unfilled cells mean no data)

Material	Compressive modulus, *MPa, **GPa	Compressive strength, MPa	Elastic modulus, *MPa, **GPa	Tensile strength, MPa	Flexural strength, MPa	Porosity %	Ultimate strain %	Strain at breaking %	Ref.
Cortical bone		100–150 <sup>a</sup> , 100–230 <sup>b</sup>	10–20 <sup>a</sup> , 16–20 <sup>c**</sup>	50–151	135–193	5–10			a – 120, b – 121, c – 122
Cancellous bone		2–12 <sup>a,b</sup>	0.1–5 <sup>a</sup> , 4.6–15 <sup>b**</sup>	1–5	10–20	50–90			a – 120, b – 122
Bacterial cellulose + collagen + apatite Silk (forced reeling)			0.27 ± 0.03 <sup>**</sup>	57.7 ± 1.8		No	21.6 ± 2.6		36
3D printed alginate/TEMPO-oxidized cellulose nanofibril hydrogel	1078–1233 <sup>*</sup>	419–455 (at strain 50%)	12.4–17.9 <sup>**</sup>	360–700		No		12–24	59 and 60
PEEK (polyether ether ketone)-based materials	2.79–3.51 <sup>**</sup>	137.11–138.63	3.79–7.37 <sup>**</sup>	95.21–101.41		Yes (3D scaffolds)			78
PLA (PLA, L-PLA, D-L-PLA)			0.35–4.14 <sup>**</sup>	15.5–150		No			85
Carbon fiber-reinforced PLA (3D printing)			256	256	210	No			106
PLGA (18% solution for electrospinning)/graphene oxide			76.3–182.7 <sup>*</sup>	2.8–6.4		No	66.9–133.6		123
PCL/HA (selective laser sintering)	1.6–1.8 <sup>*</sup>	0.7–1.3				65–70			111
PCL/HA (3D printing)		15.43 ± 1.28	80.16 ± 3.18 <sup>*</sup>			26 ± 8			113
Pearl powder/poly-amino acid composites		133–161		34–42	36–50	No			124
Polyamide 12/ZrO <sub>2</sub> /β-TCP			929.88–1286.80 <sup>*</sup>	30.63–36.60	49.87–61.75	No			119
Polyamide/HA		14.3–28.1		10.6–24.3		40–70			125

**Fig. 2** The bioactive nanoparticles/gelatin scaffolds: A – 3D model, B – the freeze-dried sample. Reprinted by permission from [62], ©Springer Nature, 2017.

To mimic the chemical composition of natural bones, Gupta *et al.* used gelatin, carboxymethyl chitin (CMC), and hydroxyapatite to prepare a gel. The  $\text{--COO--}$  groups in CMC interact with the positive ions in natural/simulated body fluids and with  $\text{Ca}^{2+}$  from HA, which is beneficial for cell proliferation and osteogenesis.<sup>64</sup> This material could be applied as a filler for small bone non-load-bearing defects or as an additive for a high-strength scaffold for enhancing osteoconductivity.

**Alginate composites.** Alginic acid, also called alginate or algin, is an anionic polysaccharide wide-spread in the cell walls of brown seaweed.<sup>65,66</sup> Venkatesan *et al.* claimed that alginate materials can be considered as promising materials for bone tissue repair due to their good scaffold-forming properties, biocompatibility, source abundance, and biodegradability.<sup>67</sup> Alginate materials are widely fabricated as microcarriers,<sup>68,69</sup> foams,<sup>70</sup> and gels.<sup>68,71,72</sup> Popescu *et al.* mixed alginate with pullulan and Si-Ca-P-Cu-O bioglass to enhance cell viability and antibacterial effect and create a bio-compatible hydrogel for supporting bone regeneration.<sup>73</sup>

In the study by Coathup *et al.*, an attempt to enhance the bone formation of granular HA was made; however, opposite results were observed: the presence of the alginate gel impeded both the formation of new bones and bone-HA scaffold contact.<sup>68</sup>

For improving the mechanical strength and degradation rate, poly(L-lactide) was added to algin and crosslinking was processed.<sup>74</sup> Shaheen *et al.* fabricated alginate/chitosan/hydroxyapatite/nanocrystalline cellulose scaffolds using a freeze-drying method and dicationic crosslinking by  $\text{CaCl}_2$ .<sup>75</sup> The obtained scaffolds had porosity over 90%, pore size of 103–230  $\mu\text{m}$ , and increased compressive yield strength (0.48–0.54 MPa compared to 0.35 MPa for chitosan/alginate samples and 0.38 MPa for chitosan/alginate/hydroxyapatite samples). The gelatin-alginate hydrogel coating onto beta-tricalcium phosphate scaffolds also exhibited maximum compressive stress of less than 0.6 MPa.<sup>72</sup>

In the study by Zheng *et al.* on silk fibroin/calcium silicate/sodium alginate scaffolds with porosity of  $\geq 75.3\%$ , the maximum compressive strength (strain = 10%) was  $< 5$  kPa.<sup>76</sup> The mechanical behavior of the composite materials mentioned above could be controlled by varying the inorganic filler amounts; however, if the amount of the filler is over a particu-

lar level, the compressive and tensile strength decrease significantly.

Leppiniemi *et al.* investigated alginate/nanocellulose hydrogels.<sup>77</sup> Abouzeid *et al.* could achieve better mechanical properties in alginate-based materials.<sup>78</sup> They fabricated alginate/TEMPO-oxidized cellulose nanofibril hydrogel scaffolds using a 3D printing method and then immersed them in a simulated body fluid for biomimetic mineralization. These hydrogel scaffolds had compressive strength in the range of 419–455 MPa at the strain of 50% and compressive modulus of 1078–1233 MPa. One can suggest that the 3D-printed alginate/TEMPO-oxidized cellulose nanofibril hydrogels may be very promising for bone substitute applications.

## 2.2 Synthetic biopolymers

As one can see, natural polymers are usually biocompatible. Also, some additional components can enhance the bioactivity of natural polymer-based composites. For example, in the study by Tong *et al.*, the cell growth and proliferation of BMSCs seeded onto silk fibroin/chitosan scaffolds were enhanced by adding the vascular endothelial growth factor (VEGF).<sup>79</sup> However, the mechanical properties of most natural polymer-based composites are insufficient for load-bearing bones. Another drawback of the natural polymers is their possible batch variation. To prevent these issues, the recombinant protein technology has been used to control monodispersity and precisely define polymer properties.<sup>80</sup>

Many newly developed polymers for medical applications are based on the combinations of natural and synthetic polymers in order to combine the great biocompatibility of natural polymers and the mechanical strength of synthetic ones. The residues of initiators, other compounds or impurities in synthetic polymers can hinder cell growth. However, most synthetic polymers have better mechanical properties and thermal stability compared to the natural ones. Also, synthetic polymers can be more easily processed into a wide range of shapes, whereas some forms are not easy to obtain for natural polymers because of the destruction of their structure during high-temperature processing.<sup>81–83</sup>

**Polyethylene materials.** In the work by Ai *et al.*, a composite material based on ultra-high-molecular-weight polyethylene (UHMWPE) was investigated. VEGF was loaded on the surface of UHMWPE by silk fibroin (SF) coating to achieve controlled release delivery.<sup>84</sup> The modified UHMWPE exhibited a better proliferation performance than raw UHMWPE: enhanced angiogenesis and osseointegration between the modified UHMWPE and the host bone. Due to the chain scission of macromolecules during the modification process, the tensile strength of UHMWPE-SF/VEGF decreased slightly (from  $1.676 \pm 0.041$  GPa for pristine UHMWPE to  $1.488 \pm 0.062$  GPa). Very strong bone substitute materials can lead to the relaxation of the surrounding bone tissues, subsequently causing bone disruption. In this regard, although this composite is very strong for use as a bone substitute material, it has a great potential for applications in anterior cruciate ligament reconstruction, and the addition

of a less strong component may lead to a composite with suitable mechanical characteristics.

**Polyether ether ketone (PEEK).** During the last few years, PEEK-based materials have been investigated for oral and cranio-maxillofacial surgery. Han *et al.*<sup>85</sup> showed that 3D-printed carbon fiber reinforced PEEK composites have great mechanical properties (tensile modulus more than 7 GPa and compressive modulus  $\sim 3.5$  GPa), which are similar to those of a cortical bone, and sufficient biocompatibility.

PEEK is bioinert, and this is a limiting factor for medical applications. Xu *et al.* reported a surface modification method to improve the biological behavior of PEEK after implantation using dexamethasone plus minocycline-loaded liposomes (with polydopamine coating before immersing in the liposome solution).<sup>86</sup> *In vitro* (hMSCs, bacterial culture seeding) and *in vivo* (C57BL/6 mice) experiments showed sufficient osteoinductive ability and cytocompatibility. To improve the biological behavior of PEEK, other surface modification methods were used: tropoelastin-functionalized plasma immersion ion implantation (the treatment provided a suitable environment for human osteoblast-like osteosarcoma cells to spread),<sup>87</sup> reinforcing by the addition of tantalum nanoparticles (besides the increase in the mechanical properties for the composites containing 3–5% Ta nanoparticles, the Ta-OH groups can cooperate with  $\text{Ca}^{2+}$  and phosphate ions for stimulating apatite nucleation),<sup>88</sup> sulfonation and further incorporation with copper nanoparticles using magnetron sputtering for improving the antibacterial and immunomodulatory ability of PEEK and creating a porous surface (Fig. 3),<sup>89</sup> fast sulfonation treatments at an ambient temperature for enhancing hydrophilicity and osteoconductivity,<sup>90</sup> neutral atom beam technology,<sup>91</sup> decoration with strontium and adiponectin,<sup>92</sup> coating with tita-

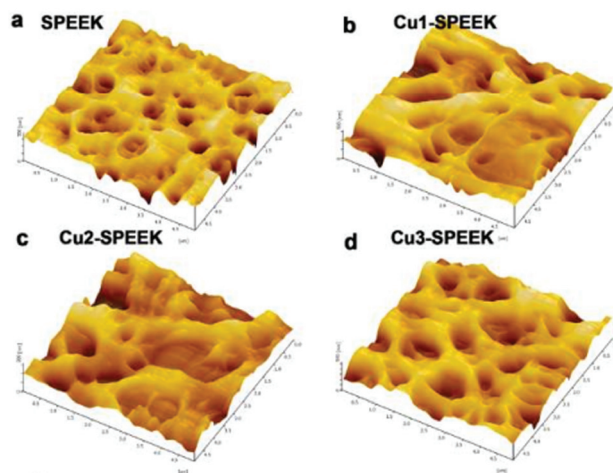


**Fig. 3** 3D atomic microscope images of: a – PEEK surface after sulfonation (SPEEK); b–d – SPEEK with different Cu contents (0.67 at%, 1.08 at% and 1.40 at% for Cu1, Cu2 and Cu3, respectively). Reprinted from ref. 83, Liu, *et al.*, *Biomaterials*, vol. 208. A surface-engineered polyetheretherketone biomaterial implant with direct and immunoregulatory antibacterial activity against methicillin-resistant *Staphylococcus aureus*. Pages 8–20, Copyright (2019), with permission from Elsevier.

nium using plasma spraying (Ti-PEEK samples showed better bone ingrowth ability compared to pure PEEK),<sup>93</sup> loading by mouse beta-defensin-14,<sup>94</sup> *etc.* Although creating a porous surface on the PEEK implant does not significantly decrease the mechanical properties of a scaffold, Deng *et al.* were concerned about the poor binding between PEEK and a surface material; thus, they preferred to equip a PEEK scaffold with a delivery system containing simvastatin, PLLA and tobramycin.<sup>95</sup> The scaffolds exhibited excellent antibacterial behaviors and osteogenic ability for MC3T3-E1.

Mei *et al.* prepared PEEK/Ta<sub>2</sub>O<sub>5</sub> composites with sand blasting treatments (to obtain a rough surface).<sup>96</sup> The compressive strength of the composites containing Ta<sub>2</sub>O<sub>5</sub> was higher compared to that of pure PEEK, and the sand blasting treatment did not decrease the compressive strength; however, the rough surface was beneficial for the biological behavior of the scaffolds (protein absorption of bovine albumin on the composite with 50 vol% Ta<sub>2</sub>O<sub>5</sub> without sand blasting was 0.75 mg g<sup>-1</sup>, and 0.94 mg g<sup>-1</sup> was observed for the composite with the same Ta<sub>2</sub>O<sub>5</sub> content but with further sand blasting treatments). Ma and Guo used popular HA as a filler for PEEK.<sup>97</sup> The tensile strength of the composites decreased significantly from 85 MPa for pure PEEK to 45 MPa for PEEK/40 wt% HA; in contrast, the elastic modulus increased by 468% and reached ~10.5 GPa. The incorporation of HA enhanced the bioactivity and osteogenesis of PEEK compared to those of UHMWPE and pristine PEEK.

The elastic modulus of PEEK-based materials is in the range of those of natural bones; thus, PEEK is expected to gain more popularity in the future for bone tissue repair.

**Poly(lactic acid) (PLA)-based composites.** Poly(lactic acid) (PLA) is a biodegradable polymer and one of the most studied biopolymers in the last years; it is used in food, packaging, medicine, and pharmaceutical industries. PLA and its co-polymer composites show excellent characteristics over other materials in tissue engineering.<sup>80,98</sup> There exist two stereoisomers of lactic acid: D,L-lactide and L,L-lactide. Furthermore, lactide can be formed by combining one D- and one L-lactide molecule, resulting in D,L-lactide.<sup>99</sup>

Kao *et al.* improved cell adhesion and promoted ECM protein secretion in 3D-printed PLA scaffolds by coating with polydopamine *via* direct immersion.<sup>100</sup> Guduric *et al.* evaluated the biological behavior of human BMSCs and endothelial progenitor cells in the 2D- and 3D-structures of PLA membranes assembled layer-by-layer.<sup>101</sup> The PLA membranes were prepared by 3D printing and were 100 µm in thickness and 200 µm in pore diameter. The microscope observations showed that the external structure and strut organization had pores of 165–375 µm. The results for the cellularized PLA membranes revealed better cell proliferation and differentiation. The layer-by-layer approach may be suitable for non-bearing bone tissues to enhance homogenous cell proliferation into the scaffold.

The PLA/10 wt% graphene oxide composite was reported as a material that can be applied as a lightweight electromagnetic interference shielding material.<sup>102</sup> The tensile properties of

the composite were higher than that reported previously for a TPU/PLA matrix:<sup>103</sup> the tensile strength was 40.2 MPa and the tensile modulus was 2454 MPa for 3D-printed samples (the fused deposition modeling (FDM) method was used). PLA is widely known as a biodegradable material, and Chen *et al.* reported the good biocompatibility of composites with graphene oxide addition; thus, the present composite<sup>103</sup> has the possibility to be applied in tissue engineering with a magnetic field as the external stimulus or in bioelectronics and biosensors, as suggested by the authors.

PLLA/collagen/hydroxyapatite composites were investigated by Zhou *et al.*<sup>104</sup> The composites containing collagen and HA had better cell viability and conductivity to cell growth and significantly higher mineralization of MC3T3-E1 cells in comparison with the PLLA and PLLA/collagen composites. However, the authors also observed lower tensile strength (2.75 MPa instead of 3.95 MPa for PLLA and 3.41 MPa for PLLA/HA) and faster degradation rate (34.5% weight loss up to 80 days compared to less than 5% for PLLA and 16.8% for PLLA/HA). The composites containing collagen and HA may be used for non-critical size defects in non-bearing places.

According to Seitz *et al.*, most of the commonly used biopolymers are biodegradable and their degradation time is not more than 1 year.<sup>105</sup> Only some biodegradable biopolymers such as polyglycolic acid (PGA), PLA, L-PLA, DL-PLA and polycaprolactone (PCL) require more than 12 months to fully degrade from a body. For serious bone injuries, especially in the case of bone diseases and the older age of a patient, a long period of time is needed to fully treat a bone fracture. Only the L-PLA tensile strength can reach 150 MPa to make L-PLA applicable as a bone substitute material,<sup>105</sup> and the data from Van de Velde and Kiekens (Table 1) show the same information.<sup>106</sup>

Besides applications as scaffolds, the PLA-based materials may be used as microcarriers for tissue cell-based therapy due to the controllable degradation rate and biocompatibility of PLA. This field still needs to be investigated further.<sup>99</sup>

**Poly(lactic-co-glycolic acid) (PLGA).** PLGA is a copolymer of glycolic acid and lactic acid.<sup>98</sup> Since PLGA contains both PLA and PGA, its degradation rate depends on the ratio of monomers and can vary from months to years. The degradation rate also depends on molecular weight, shape, structure, and porosity.<sup>80</sup>

The pure PDLGA samples obtained by compression molding showed a high value of elastic modulus, *i.e.*, about 1.2 GPa, which suddenly dropped after reaching the yield point during tensile strength tests; thus, PDLGA scaffolds are brittle.<sup>107</sup> When PDLGA was mixed with L-lactide-co-ε-caprolactone, the samples showed a more plastic behavior; however, the elastic modulus and yield strength values were significantly lower: 7.1–650 MPa elastic modulus and 5.6–28 MPa yield strength for the composites with 20–80% L-lactide-co-ε-caprolactone components.

In the study by Wu *et al.*, PLGA/graphene nanoplate composites were investigated.<sup>108</sup> The results of seeding rat BMSCs on the films revealed accelerated differentiation, enhanced adhesion and better guiding bone regeneration properties.

Namini *et al.* used PLGA to create composites with HA using both electrospinning and freeze-drying methods.<sup>109</sup> The seeding of human endometrial stem cell (hEnSC)-derived osteoblast-like cells onto the PLGA/HA samples revealed that the results for the freeze-dried composites were better than those for the electrospun ones. The freeze-dried samples were more porous, and the cell viability was higher compared to that of the samples made by electrospinning. The good adhesion and proliferation of cells make the PLGA/HA composites made by the freeze-drying method excellent candidates for applications in bone regeneration.

Park *et al.* proposed a composite material containing poly(D,L-lactic-co-glycolic acid) (PDLGA) and magnesium hydroxide (MH).<sup>110</sup> The porous scaffolds of PDLGA/MH were obtained by the freeze-drying method using ice particles as porogens. The diameter of the MH particles was 80–200 nm and the scaffold micropores were in the range of 30–70  $\mu\text{m}$ . The composite scaffolds showed enhanced chondrogenesis markers, reduced calcification and reduced release of inflammatory cytokines in comparison to the PLGA scaffolds. The MH-containing scaffolds supported the healing of osteochondral defects in rats. The authors suggested the potential application of the PDLGA/MH composites for cartilage and other soft tissue regeneration.

Luo *et al.* fabricated PLGA nanofiber scaffolds doped with graphene oxide (GO) using the electrospinning method.<sup>111</sup> The porous structure and fiber diameter were similar to those of natural extracellular matrices. Doping by GO facilitated cell attachment and proliferation but decreased the mechanical parameters such as the breaking strength and Young's modulus. The authors reported that GO cannot bear the stress, leading to decrease in the breaking strength. Nanofibrous mats<sup>111</sup> showed excellent hemocompatibility and cell proliferation; the addition of GO accelerated stem cell differentiation and increased osteocalcin production. Thus, the GO-doped PLGA composites may be promising as biodegradable materials for bone regeneration in non-bearing applications due to their weak mechanical properties (tensile stress in the range from  $2.8 \pm 0.3$  MPa for 15% PLGA to  $5.7 \pm 0.7$  MPa for 18% PLGA).

**Polycaprolactone.** Marei *et al.* investigated PLA- and PCL-based nanofibrous samples (fabricated by the electrospinning technology) to enhance the interaction between stem cells and scaffolds.<sup>112</sup> To evaluate the feasibility of applying these scaffolds for bone tissue repair, the adhesion and proliferation of two types of stem cells (BMSCs and adipose tissue stem cells, ASCs) were investigated. BMSCs and ASCs attached to both the PCL and PLA fibers and retained their cytoskeletons, but ASCs cultured on PLA nanofibers exhibited low cell viability. The authors considered further optimizations by varying electrospinning parameters and using additional treatment methods.

In the work by Du *et al.*, porous PCL/HA composites were obtained by microsphere-based selective laser sintering.<sup>113</sup> The scaffolds exhibited a controlled microstructure and porosity, excellent histocompatibility, and enhanced proliferation

and differentiation of MSCs *in vitro*. This work proved that the micropores created by the microspheres of about 100  $\mu\text{m}$  provide appropriate surfaces for cell adhesion, spread and ingrowth.<sup>113</sup> The PCL/HA composites promoted angiogenesis in comparison to pure PCL scaffolds, but it was shown that the compressive modulus decreased from 3.1 MPa for the PCL scaffold to 1.6 MPa for the composite containing 20% hydroxyapatite (HA). The compressive strength was much lower than those of cortical or cancellous bones.

There was an attempt to reinforce PCL by the addition of silica nanoparticles and create a cytocompatible composite membrane as a physical barrier for preventing fibroblasts from moving to the wound, preserving space for new bone tissues.<sup>114</sup> The PCL/Si-NP membranes were cytocompatible and exhibited improved biofunctional properties. The addition of 25–50 wt% silica nanoparticles to the PCL (100 wt%) matrix increased the tensile strength and tensile modulus of composites (2.9 and 9.5 MPa, respectively, for pure electrospun PCL; 5.8 and 13.5 MPa for the composites with a 50 : 100 Si-NP : PCL ratio). Further addition (up to 75 wt%) was not beneficial for the mechanical properties of the PCL/Si-NP composite materials.

Hendrikson *et al.* showed that the more the PCL molecular weight, the better the mechanical properties of a scaffold.<sup>115</sup> The stiffness measured during the unconfined compression test was 204.2 MPa for a higher molecular weight of PCL ( $M_w = 65\,000$ ) and 147.5 MPa for a lower molecular weight of PCL ( $M_w = 14\,000$ ).

The composite of poly(L-lactide-co- $\epsilon$ -caprolactone) prepared by the compressive molding method showed small elastic modulus only of 3.2 MPa; however, the strain at rupture was 937% and the stress at rupture was 19 MPa.<sup>107</sup>

Goncalves *et al.* proposed the use of carbon nanotubes (CNTs) as a component responding to external stimuli for accelerating the healing process.<sup>116</sup> It was expected that electrical stimulation after material implantation would induce osseointegration. Among the PCL/HA/CNT composites with 0–10 wt% CNTs, the samples with 0.75 wt% CNTs showed the best mechanical behavior, but these samples were not electrically conductive. The best combination of electrical conductivity and mechanical properties was shown by the samples with 2 wt% CNTs. The compressive yield strength was about 4 MPa and the elastic modulus was 44 MPa, which was in the range of the values for trabecular bones. However, CNTs could not be used as a reinforcing agent for composites: CNTs may enhance electrical conductivity, but the mechanical behavior can worsen. The mechanical properties of PCL/HA/2–10 wt% CNTs were worse than those of the PCL/HA samples.

**Other materials for bone tissue engineering.** In this subchapter, we have reported other less popular materials supposed to be applied in bone tissue repair.

Poly(3-hydroxybutyrate-co-4-hydroxybutyrate) co-polymer (P34HB)/poly(ethylene glycol) (PEG) nanofiber membranes were prepared by the electrospinning technology by Wang *et al.*<sup>117</sup> The mechanical and biological properties increased compared to those of pure P34HB (weak mechanical properties

of P34HB were also introduced by Yang and Cai);<sup>118</sup> however, this composite is not suitable for load-bearing applications.

Wu *et al.* investigated pearl powder/poly-amino acid (P/PAA) composites for load-bearing bone repair.<sup>119</sup>

The samples with 0–50 wt% pearl powder exhibited 100–161 MPa compressive strength, 27–42 MPa tensile strength, and enhanced mineralization ability due to the interaction between  $\text{Ca}^{2+}$  from pearl and  $\text{PO}_4^{3-}$  from SBF, which is a trigger for apatite nuclei formation. The degradation experiments showed only 1.46–3.64% weight loss after 28 days in PBS; thus, the P/PAA composites may be used for the repair of critical bone defects.

Mills *et al.* doped several types of antibiotics (gentamicin sulfate, tobramycin, and nitrofurantoin) into poly(methyl methacrylate) (PMMA).<sup>166</sup> The results showed that antibiotic-doped PMMA could prevent osteomyelitis by inhibiting the bacterial activity through antibiotic release.

Hydroxyapatite/poly xylitol sebacic adipate/vitamin K composites were investigated by Dai *et al.* for applications in bone repair.<sup>167</sup> The weight loss after 28 days in PBS at 37 °C was about 28%, which is critical for repairing defects in load-bearing bones. This type of material is supposed to stimulate bone formation in non-critical defects.

Previously reported polyamide composites were discussed as potential bone substitute materials. Nano-hydroxyapatite/polyamide 66 (especially doped by peptide D-RADA16-RGD),<sup>168</sup>  $\text{ZrO}_2/\beta\text{-TCP}$ /polyamide 12,<sup>125</sup> and porous polyamide/HA composites prepared by selective laser sintering<sup>126</sup> exhibited sufficient bioactivity and cytocompatibility, but the mechanical behavior of these composites still needs to be improved (Table 1).

Zhang *et al.* prepared porous scaffolds from polyetherimide (PEI).<sup>169</sup> Although the compressive modulus of the porous scaffolds was lower than that of pure PEI (78.95 and 1376.61 MPa, respectively), the modulus of porous PEI was in the range of the values for natural cancellous bones.

Poly(acrylonitrile butadiene styrene) (ABS)<sup>165</sup> and its composite with silver nanoparticles<sup>170</sup> showed great mechanical properties (elastic modulus more than 1.6 GPa; tensile strength more than 44 MPa), sufficiently low cytotoxicity and Hs680.Tr (human tracheal fibroblast) and Saos-2 (human osteosarcoma) cell viability.

Several poly(glycerol-sebacate) (PGS)-based materials were reported recently. PGS-co-PEG polymers with PEG contents of 20–40% exhibited weak tensile stress (168–801 kPa), weak Young's modulus (183–668 kPa), and very fast degradation (20–50% weight loss after 21 days in a Tris-HCl solution), which led to the rapid loss of the mechanical support in a wound side.<sup>171</sup> The addition of  $\beta\text{-TCP}$  into PGS also did not significantly increase the mechanical properties (0.21 MPa tensile strength and 1.95 MPa Young's modulus).<sup>172</sup> A biocompatible PGS/PCL blend was reported by Salehi *et al.* and was proposed for cornea tissue engineering.<sup>173</sup> One can suggest that the PGS-based biopolymers are more suitable for soft tissue repair than for bone repair.

To sum up the sections 2.1–2.2, some significant data have been collected in Table 1. As one can see, most natural and

synthetic biopolymers cannot reach the range of the mechanical strength of natural bones.

The addition of reinforcing components and supplementary treatments may lead to the enhancement in the mechanical and biological performances of a material. However, it is important to find a balance among degradation rate, porosity, and mechanical properties.

In the subsequent sections, other groups of synthetic polymers will be discussed but first, the manufacturing methods of polymer materials should be reviewed.

## 2.3 Manufacturing methods for bone substitute materials.

### Materials for rapid prototyping technology

For the purpose of this section, the popular technologies for making polymer scaffolds are summarized in Table 2.<sup>174</sup>

As can be seen, all fabrication methods have their limiting factors. Nowadays, polymer-based composites fabricated by rapid prototyping (RP) methods are gaining popularity.<sup>163</sup> The use of 3D printers increases the speed of production and lowers one-of-a-kind product cost<sup>175</sup> because there is no need to adjust the manufacturing equipment to create a new implant; only the STL-file on a computer program must be adjusted. Also, only the RP method allows the creation of scaffolds with any kind of pore size and configuration. The difficulty of scaffold configuration is defined only by application requirements and the skills of an operator for drawing 3D models.

There exists no technology without drawbacks, and the RP technology has several drawbacks (Table 3).

As one can see, RP methods (especially, the FDM technology) have great promise for bone substitute applications because of RP's ability to mimic the complex structure of a natural bone. Han *et al.* used a 3D printer for carbon fiber-reinforced PEEK (CFR-PEEK) composites, and the authors claimed that the RP technology is a more appropriate method for matching CFR-PEEK composites to mimic human bones and avoid stress shielding.<sup>85</sup>

Murphy *et al.* investigated PCL/13-93B3 (bioactive borate glass) composites.<sup>176</sup> The scaffolds were fabricated by the 3D-printing method and pores from 100 to 300  $\mu\text{m}$  were obtained, which are beneficial for bone growth.<sup>177</sup> The scaffolds showed a controllable release of 13-93B3 glass over a period of 2 weeks into minimum essential medium alpha modified ( $\alpha\text{-MEM}$ ): about 70% of the 13-93B3 borate glass reacted in 14 days. This makes the scaffold material beneficial in drug delivery applications.

However, the rapid degradation rate of a scaffold material is not preferable for bone substitute materials for elderly people and people with bone diseases due to their low bone renewing speed, and the quick biodegradation of borate bioglass can lead to the decreased mechanical properties of the scaffold; thus, the scaffold cannot support the weight of an adult patient after 2 weeks.

In the work of Wu *et al.*,<sup>185</sup> polyhydroxyalkanoate/wood flour (PHA/WF) and maleic anhydride (MA)-grafted (PHA-g-MA)/WF composites were investigated. The PHA-g-MA/WF

**Table 2** Methods of polymer scaffold fabrication

Method	Advantages	Disadvantages	References
Solvent casting/particle leaching	<ul style="list-style-type: none"> <li>- Porous structures can be produced</li> <li>- Simplicity, no requirement of any special equipment</li> </ul>	<ul style="list-style-type: none"> <li>- Porosity leads to significant loss of mechanical properties</li> <li>- Possible difficulty with leaching particles</li> <li>- Residues of organic solvents may have toxic effects</li> </ul>	127–133
Thermally induced phase separation	<ul style="list-style-type: none"> <li>- Ability to control pore size and structure</li> </ul>	<ul style="list-style-type: none"> <li>- It is not easy to achieve pore sizes more than 200 <math>\mu\text{m}</math></li> <li>- It is difficult to adjust micro- and macrostructure of sample</li> </ul>	134–138
Melt molding (injection molding, compression molding)	<ul style="list-style-type: none"> <li>- Structures of varying shapes and sizes can be produced</li> <li>- Does not require organic solvents</li> </ul>	<ul style="list-style-type: none"> <li>- With nonporous layers on the surface, it is difficult to leach particles and porogen compounds</li> <li>- Requires high operating temperatures</li> </ul>	139–146
Electrospinning	<ul style="list-style-type: none"> <li>- Ease of control over the physical morphology</li> </ul>	<ul style="list-style-type: none"> <li>- Small pore size</li> <li>- Small thickness of nanofibers</li> </ul>	138, 147–151
Hydrogels	<ul style="list-style-type: none"> <li>- No requirement of any special equipment</li> <li>- Does not require solvent</li> </ul>	<ul style="list-style-type: none"> <li>- Low mechanical properties, not for load-bearing applications</li> <li>- Gel shrinkage because of the loss of water</li> </ul>	152–156
Gas foaming	<ul style="list-style-type: none"> <li>- Porosity is easily controlled</li> <li>- Does not require organic solvents</li> </ul>	<ul style="list-style-type: none"> <li>- It is difficult to control pore size and interconnectivity</li> <li>- Low mechanical properties, not for load-bearing applications</li> </ul>	133, 157–160
Emulsion freeze drying	<ul style="list-style-type: none"> <li>- Ability to control pore sizes and interconnectivity</li> <li>- Requires less solvent</li> <li>- No need for time-consuming processes (drying or porogen leaching)</li> </ul>	<ul style="list-style-type: none"> <li>- Emulsions may be unstable, require additional surfactants</li> <li>- Low mechanical properties, not for load-bearing applications</li> <li>- Requirements to a filament</li> </ul>	138, 161, 162
Rapid prototyping (3D printing, selective laser sintering, stereolithography (SL), fused deposition modeling (FDM), PolyJet)	<ul style="list-style-type: none"> <li>- Ability to create low-volume or one-of-a-kind parts based on patient-specific needs</li> <li>- Geometrical freedom (complex-shaped functional implants)</li> </ul>	<ul style="list-style-type: none"> <li>- Inability to manufacture multicomponent structures</li> <li>- Surface roughness cannot be controlled</li> </ul>	138, 152, 163–165

**Table 3** Advantages and disadvantages of RP technology

Technology	Advantages	Disadvantages
3D-printing	Comfort for a patient (individually shaped implants); speed; <sup>178</sup> pore size control; no need for solvents (excl. SL method) or toxic reagents; complex geometries	Complex scaffolds
FDM		Large variation of applicable polymers
SL		<ul style="list-style-type: none"> <li>The liquid binder can lead to toxicity of a scaffold; Loose powder; Requires cleaning after printing; The nozzle size limits the scaffold resolution<sup>179</sup></li> <li>Problems occurring during printing process (a failed print or a print not matching its STL-file);<sup>180,181</sup> Requirements of the filament (diameter, ductility)</li> <li>Limited types of photopolymerizable materials are available;<sup>179</sup> Newly printed parts have to be washed, cured, and dried because they are sticky and messy;<sup>182</sup> The SL equipment is more expensive than the FDM one; process costs are quite expensive<sup>183</sup></li> </ul>
SLS		Minimized use of excess polymer powder
PolyJet		Layer resolution, printing precision <sup>165</sup>

samples showed better mechanical behaviors, water resistance, and antibacterial activity and higher quality of 3D-printed strips than the PHA/WF samples. The tensile strength at failure could reach  $\approx 26$  MPa for PHA-g-MA/40 wt% WF, and the antibacterial properties improved with the addition of 20 wt% WF.

The same authors<sup>185</sup> also investigated PHA-g-MA/TPF (a coupling agent-treated palm fibre) composites.<sup>186</sup> The composites were nontoxic and exhibited good water resistance. Although the tensile strength at break could reach  $\approx 23$  MPa for the composite with 20 wt% TPF, rapid weight loss and high degradation rate were observed. The biodegradation rate increased with the addition of PF or TPF; the composite with 40 wt% TPF degraded quickly over the first 30 days. The applications of both materials as bone substitutes are limited by their degradation speed and very high water resistance. However, the PHA-based composites can be potentially used as environment-friendly biomaterials.

In the article by Filgueira *et al.*, biocomposites containing PLA and wood pulp fibers were investigated.<sup>187</sup> The thermo-mechanical pulp (TMP) was modified by the laccase-assisted grafting of octyl gallate (OG) and lauryl gallate (LG) to achieve strong biomaterials with low water absorption rates. The strength of most composites was lower compared to that of pure PLA, which can be caused by a porous structure, insufficient homogeneity, and poor fiber-matrix interaction and fiber dispersion in the PLA matrix (this can lead to fiber agglomeration and initiate failure and crack propagation). Only one filament sample with 90% PLA and 10% OG-modified TMP showed the tensile strength of about 58 MPa, and the samples with 10 and 20% TMP (OG-modified) showed higher values of maximum force in comparison with the PLA filament. The tensile strength of 3D-printed dog bones was lower than that of the one made of PLA prepared by the traditional methods. Although the PLA/TMP composites have some difficulties with respect to mechanical properties, the authors suggest that the use of OG-treated wood pulp fibers for antibacterial devices can be extended.

The biological effect of FDM-printed PLA on osteoblasts *in vitro* was investigated by Wurm *et al.*<sup>188</sup> The results of seeding human fetal osteoblasts (hFOB 1.19) revealed high viability, homogenous covering of the sample surface and good cell proliferation; no cytotoxic effects were observed. The Young's modulus was  $3.2 \pm 0.4$  GPa for PLA bulk sample created by FDM; this was the lowest value for cortical bones (3.3–20 GPa) and was within the range for trabecular bones (0.76–10 GPa), as reported by Mow and Huiskes.<sup>189</sup> The authors claimed that PLA is an attractive material for reconstructive surgery and very appropriate for maxillofacial applications. The FDM method does not alter the biocompatibility of PLA, and one of the advantages of FDM is the possibility to make individually shaped scaffolds, which can decrease the psychological strain on a patient.

**Polyurethanes.** Parisi *et al.*,<sup>190</sup> Xu *et al.*<sup>35</sup> and Chung *et al.*<sup>174</sup> claimed that although polyurethanes (PU) require a complicated and expensive manufacturing process, the application of

PU in the biomedical field is growing dramatically due to their toughness, biocompatibility and hemocompatibility. The authors also suggested the promising applications of PU as a material for long-term implants and as a scaffold for different types of tissues.<sup>191</sup>

In the study by Guo *et al.*, reactive polyurethane (PUR) scaffolds were fabricated using the t-FDM (new template-fused deposition modeling) process.<sup>192</sup> The pore size of the PUR scaffolds was adjusted by changing the diameter of the sacrificial fibers, which were removed by dissolving after pouring PUR into the templates and curing. The results of measuring substrate modulus (the method of Oliver and Pharr<sup>193</sup> was used) showed that the modulus of t-FDM-manufactured PUR scaffolds (10–900 MPa) is within the ranges of those of trabecular bones (93–365 MPa) and cortical bones (871–11 500 MPa).<sup>194</sup>

Tsai *et al.* made a complete adult tracheal construct using the FDM technique.<sup>195</sup> As a material, the authors chose a mixture of TPU: a polyester (polycaprolactone) polyol-based and a polyether polyol-based material. The mechanical properties of the tracheal sample were sufficient, and the authors suggested that the 3D printing technology is a very promising technology for tissue engineering, especially for TPU materials, due to low price and ease of processing.

Chen *et al.* fabricated TPU/PLA/GO composites (Fig. 4).<sup>103</sup> Graphene oxide significantly improved the mechanical properties of a TPU/PLA (7 : 3) matrix: the compressive modulus reached to about 145 MPa for the composite with 5 wt% GO, and the tensile modulus reached 80 MPa for the composite with 0.5 wt% GO. The effect of printing orientation on mechanical properties was also shown and the differences can be explained by the formation of large/small voids between layers. The results of seeding by NIH3T3 mouse embryonic fibroblast cells revealed good cell viability, and a small amount of graphene oxide was preferable for cell proliferation. Although the mechanical properties of the composites increased by the addition of graphene oxide, they were not sufficient for applications as bone substitutes, and the fabricated specimens did not meet the requirement of the controlled porosity of a material. However, the TPU/PLA/GO com-



**Fig. 4** The TPU/PLA/GO scaffold after FDM printing. Reprinted with permission from Q. Chen, *et al.*, 3D printing biocompatible polyurethane/poly(lactic acid)/graphene oxide nanocomposites: anisotropic properties, *ACS Applied Materials & Interfaces*, 2017, 9(4), 4015–4023.<sup>103</sup> Copyright (2017) American Chemical Society [103].

posites can be used as promising materials for bioengineering due to their great biocompatibility.

Polyurethanes have limited biocompatibility, cytocompatibility and hemocompatibility; thus, their performance for inner-body applications must be enhanced by the addition of other components and various fabrication techniques.<sup>196</sup> Taking this into account, Chung *et al.* offered several ways to impart an antibacterial behavior to PUs; this involved modifying the PU surface, using antimicrobial agents or a copolymer with specific properties, *etc.*<sup>174</sup> Some examples of enhancing the cytocompatibility and antibacterial activity of PU scaffolds are discussed in section 2.3.

#### 2.4 Shape memory polymers for bone implants

The serious drawback of biopolymers as a material for bone implants is their mechanical properties. Soft polymers cannot be used for load-bearing bone scaffolds. Hence, it is necessary to create polymers with high mechanical properties as bone substitutes. Some attempts for creating a strong polymer composite material have been made recently, including the very promising experiments in the field of polymers with the shape memory effect (SMP).<sup>197,198</sup>

SMP is a so-called smart material that has the ability to regain its permanent shape from a deformed state under external stimuli such as heat, electric/magnetic field, light, solvent exposure, and water immersion. In contrast to the traditional polymer materials and alloys with the shape memory effect, SMPs have significant benefits:

1. In comparison to Ni-Ti shape memory alloys and stainless steel and Co-Cr-based alloys frequently applied for bioimplants, there is no metal ion release from SMP implants.<sup>199,200</sup> The release of Ni, Cr, *etc.* ions can cause allergic reactions and cytotoxicity<sup>201,202</sup> and is associated with a risk for diseases including cancer.<sup>203</sup>
2. Several external stimuli such as heat, light, magnetic field, and solvent exposure can trigger relaxation.
3. The self-healing effect<sup>204</sup> under load can prolong the service life of an implant.<sup>205</sup>
4. The most important benefit is the possibility to create deploying structures that can minimize surgical invasiveness. Deployable implants are fully porous to allow new bone ingrowth (Fig. 5).<sup>206,207</sup>

Lately, many studies based on biomaterials having shape memory properties have been published.

Tian *et al.* proposed a new method of manufacturing tough carbon fiber-reinforced PLA composites.<sup>123</sup> It involves additional manufacturing stages such as recycling and remanufacturing to enhance the bonding and permeation between fiber and matrix and to achieve excellent interfacial properties. The mechanical properties of this composite material are outstanding, and it is very promising for applications where a degradable “green” material is needed; however, for using this material as a bone substitute, the possibility of making this material porous needs to be considered.

In the work by Arnebold and Hartwig, an epoxy-based SMP composite was presented.<sup>208</sup> Poly( $\omega$ -pentadecalactone) (PPDL)

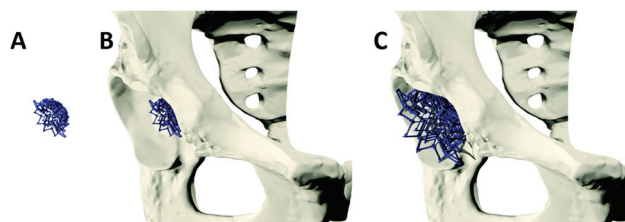


Fig. 5 Deployable bone implant: A – retracted implant; B – implanted inside the body; C – deployed inside the body. Reproduced from ref. 206 with permission from the Royal Society of Chemistry, copyright 2018.

and poly( $\epsilon$ -caprolactone) (PCL) were polymerized. The epoxy/PPDL sample exhibited fast shape fixity, sufficient shape memory cycle stability, and enhanced strength and toughness (due to heterogeneous morphology as a result of segregation and crystallization) in comparison with the epoxy/PCL samples.

Recently, some authors reported biocompatible hydrogels with the shape memory effect. Gupta *et al.* fabricated anion-controlled shape-memory hydrogels using Nvj-1 (histidine-rich jaw proteins taken from marine sandworms *Nereis virens*).<sup>209</sup> It was found that exchanging anions could modulate the interaction of Zn with the Nvj-1 protein, increase stiffness and adjust viscoelastic properties. Silk fibroin bioinks also demonstrated the shape memory feature.<sup>210</sup>

The enzymatically cross-linked silk hydrogels had 59.1% porosity, and the compressive stress at 50% strain was about 0.25 MPa; this value was very similar to that for human meniscus (Fig. 6). Cation-triggered polyacrylamide/carbomethyl cell-

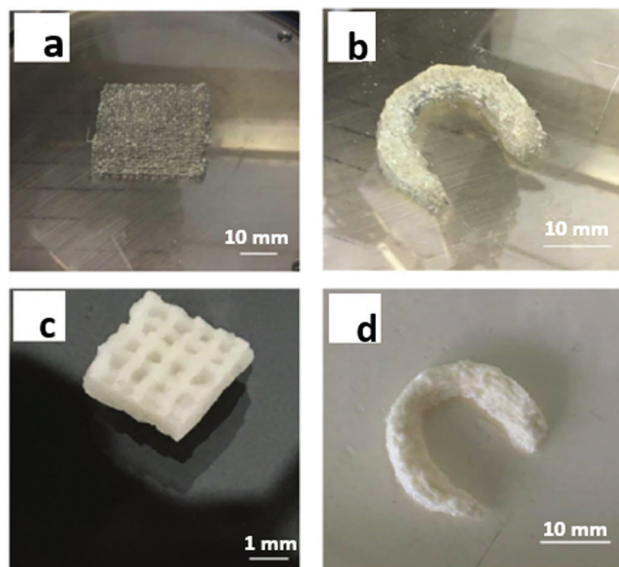


Fig. 6 Silk fibroin 3D-printed scaffolds: (a) cube-shaped 3D scaffold; (b) meniscus implant before freeze-drying; (c) cube-shaped scaffold after freeze-drying; (d) meniscus implant after freeze-drying treatment. Reproduced from ref. 210 with permission from Wiley, copyright 2017.

ulose (PAM/CMC) hydrogels were synthesized by Li *et al.*<sup>211</sup> After immersion in FeCl<sub>3</sub>, the PAM/CMC-Fe<sup>3+</sup> hydrogel exhibited shape fixity ratio of 95% and tensile strength at break of 1.23 MPa. Chitosan/graphene oxide (CS/GO) hydrogels showed a pH-driven shape memory effect.<sup>212</sup> CS/5 wt% GO had the best mechanical properties among the prepared hydrogels, which were similar to those of a natural costal cartilage. It was shown that the mechanical behavior of hydrogels can be controlled by adjusting the crosslinking parameters. However, the mechanical strength of the hydrogels was still not sufficient for load-bearing applications such as in bone substitutes.

In view of the work by Ban *et al.*,<sup>213</sup> it can be expected that polyurethane-based materials can be one of the most promising materials in bone tissue engineering. In this work, polyethylene glycol-based shape memory polyurethane (SMPU) was incorporated by 4-octyldecyloxybenzoic acid (OOBA) and a liquid-crystalline SMPU (LC-SMPU) was obtained. The LC-SMPU composites had triple-shape memory properties and self-healing ability; also, the storage modulus was above 200 MPa at indoor temperatures and above 100 MPa at the inner-body temperature (37 °C). There is no information about the biocompatibility of the LC-SMPU composites, but it must be considered that the polyurethane-based materials can achieve high mechanical properties through the addition of potential crystallization centers in polyurethanes.

The 3D-printed porous scaffolds made from aromatic shape memory polyurethane DiAPLEX MM3520 showed both cytocompatibility and good recovery of the permanent shape.<sup>214</sup>

One of the most comprehensive studies during the last 4 years is the work by Deng *et al.* on an electroactive biodegradable shape memory copolymer.<sup>215</sup> The copolymer of PCL and amino-capped aniline trimer combined together by hexamethylene diisocyanate using facile synthesis showed great elasticity (elongation at break 646–1331%), adjustable recovery temperature around the human inner-body temperature, excellent shape memory properties (fixity ratio 61.1–77.8%, recovery ratio 100%), and significantly improved biological behavior of C2C12 cells in comparison to neat PCL. PCL with a molecular weight of 3000 was used for mechanical measurements due to its recovery temperature being most suitable to the human body. The mechanical and cell seeding results showed that decreasing aniline trimer led to better proliferation, increased degradation rate, increased Young's modulus (due to various crystallization abilities), and increase in elongation at break (due to mobility and slip between macromolecular chains). Despite the great shape memory effect and appropriate mechanical strength (tensile stress in the range of 37.3–48.3 MPa), this PCL-AT copolymer degraded faster than that required for bone recovery: the samples lost 10–50% of their weight within 36 hours. The PCL-AT copolymer is more suitable for soft tissue engineering.

Kawaguchi *et al.* used chitosan fibers (biomass nanofibers, BiNFi-s) to improve the antibacterial properties of polyether-based thermo-plastic polyurethane (TPU).<sup>216</sup> The composite with 5 wt% BiNFi-s exhibited increase in the elastic modulus by 40% compared with plain TPU. The composites with 2 and

5 wt% BiNFi-s exhibited shape recovery with clinically significant changes in temperature; the yield strength had no significant changes. The X-ray diffraction results showed that the TPU samples were semicrystalline, and the TPU/BiNFi-s composites had an amorphous structure. There is a risk of the weakening of hydrogen bonds between N–H and C=O groups because of water absorption in thermo-responsive SMP (especially with an amorphous structure), which can lead to decrease in glass transition temperature.

Tan *et al.* improved the hydrophilicity and biological properties (antibacterial activity, cytocompatibility, and infection prevention ability) of shape memory PU by adding chitosan and gelatin and further soaking in AgNO<sub>3</sub>.<sup>217</sup> The SMPU-based composite had a porous structure, tensile stress of about 3.5 MPa (at 30% strain), and satisfactory biological behavior. The authors suggested this material for smart wound treatment but not as a bone material due to the poor mechanical properties for bone substitute applications. However, this study showed that the biological behavior of PU-based materials can be controlled by the addition of antibacterial agents.

Shape memory polymers have been widely investigated over the last years. There are still some problems, such as degradation rate, mechanical strength, cytocompatibility and antibacterial response of a material. However, SMPs belong to the unique type of smart programmable materials, and their self-healing effect and the possibility to decrease surgical invasiveness by creating deployable structures should be taken into account. SMPs are very promising materials for biological applications including their use as bone substitute materials with controllable properties.

### 3. Conclusions

In the field of bone substitute materials, recent studies have focused on bioactive and/or biodegradable materials, including bioactive ceramics, polymers and biodegradable metals.

Both synthetic and natural polymer materials and their organic/organic and organic/non-organic composites have demonstrated promise for bone tissue engineering.<sup>218</sup> Biopolymers proved their biocompatibility during experiments with mice, rabbits, dogs or even people. The examples include PLA,<sup>219</sup> PLGA,<sup>220</sup> poly(methyl methacrylate),<sup>221</sup> chitosan,<sup>222</sup> poly(hydroxybutyrate), PCL, proteins (silk, collagen),<sup>223</sup> and poly(ethylene glycol) diacrylate (PEGDA) hydrogels.<sup>224</sup> A brief review of the research directions in biopolymers during the last few years was presented.

Biopolymers exhibit relatively high toughness and plasticity and their behavior may be controlled by the molecular design and manufacturing technologies. In spite of a good combination of basic properties, there is contradiction among the mechanical properties, porosity and biodegradation rate.<sup>34</sup> It is obvious that the factors beneficial for cell growth and proliferation (for example, high porosity and pore interconnectivity) are inconsistent with high mechanical properties. This

conflict makes creating the ideal bone substitute material a time-consuming and challenging process.

As one can see, a pure biopolymer cannot meet all the requirements for bone substitute materials;<sup>106</sup> thus, recent research has aimed to combine different types of bone biomaterials and create polymer-based composite materials, in which the advantages of each material type can be combined, for example, biopolymer-reinforced 45S5 bioglass scaffolds,<sup>225</sup> nano-hydroxyapatite/collagen composites,<sup>226</sup> gelatin-bioactive glass hybrid scaffolds,<sup>227</sup> gelatin/siloxane hybrid composites,<sup>228</sup> etc.

The authors of this article suggest that shape memory biopolymers have a great future in the field of artificial bones because of their ability to change shape under specific conditions, which can make a patient feel more comfortable with an implant and reduce surgical intervention.

In the article, it was shown that the rapid prototyping technology has advantages, such as the possibility to build complex scaffolds, easily adjusted files for printing one-of-a-kind implants for patients, and avoiding toxic reagents during the manufacturing process.

An ideal bone substitute material can be created by the further investigation of the interactions between a bone substitute material and body cells using cutting-edge technologies and researchers' collaboration.

## Conflicts of interest

There are no conflicts to declare.

## Acknowledgements

The authors would like to acknowledge the financial support of the National Natural Science Foundation of China (Grant No. 11632005 and 11672086).

## References

- 1 Bone diseases, MedlinePlus, 2016, <https://medlineplus.gov/bonediseases.html>, (accessed March 2019).
- 2 T. Meling, K. Harboe and K. Soreide, Incidence of traumatic long-bone fractures requiring in-hospital management: A prospective age- and gender-specific analysis of 4890 fractures, *Injury*, 2009, **40**(11), 1212–1219, DOI: 10.1016/j.injury.2009.06.003.
- 3 Prevent Falls and Fractures, National Institute on Aging, 2017, <https://www.nia.nih.gov/health/prevent-falls-and-fractures>, (accessed December 2018).
- 4 10 facts on ageing and health, World Health Organization, 2017, <http://www.who.int/features/factfiles/ageing/en/>, (accessed February 2019).
- 5 A. C. Looker, N. S. Ishafani and J. A. Shepherd, FRAX-based Estimates of 10-year Probability of Hip and Major Osteoporotic Fracture Among Adults Aged 40 and Over: United States, 2013 and 2014, *NHSR*, 2017, **103**, 1–13.
- 6 Bone grafting, Wikipedia, [https://en.wikipedia.org/wiki/Bone\\_grafting](https://en.wikipedia.org/wiki/Bone_grafting), (accessed January 2019).
- 7 P. Klokkenvold and S. Jovanovic, Advanced Implant Surgery and Bone Grafting Techniques, in *Carranza's Clinical Periodontology*, ed. M. G. Newman, H. H. Takei and F. A. Carranza, W.B. Saunders, Philadelphia, 2002, pp. 907–908.
- 8 Bone grafts: New developments, Wang, J.C., 2017, <https://www.spineuniverse.com/exams-tests/bone-grafts-new-developments>, (accessed February 2019).
- 9 C. R. Lareau, *et al.*, Does autogenous bone graft work? A logistic regression analysis of data from 159 papers in the foot and ankle literature, *Foot Ankle Surg.*, 2015, **21**(3), 150–159, DOI: 10.1016/j.fas.2015.03.008.
- 10 A. L. Dumitrescu, Bone grafts and bone graft substitutes in periodontal therapy, *Chemicals in Surgical Periodontal Therapy*, 2011. DOI: 10.1007/978-3-642-18225-9\_2.
- 11 N. Shibuya and D. C. Jupiter, Bone Graft Substitute: Allograft and Xenograft, *Clin. Podiatr. Med. Surg.*, 2015, **32**(1), 21–34, DOI: 10.1016/j.cpm.2014.09.011.
- 12 M. Bahraminasab and B. B. Sahari, NiTi Shape Memory Alloys, Promising Materials in Orthopedic Applications, in *Shape Memory Alloys – Processing, Characterization and Applications*, *InTech*, 2013. DOI: 10.5772/2576.
- 13 X. P. Tan, *et al.*, Metallic powder-bed based 3D printing of cellular scaffolds for orthopaedic implants: A state-of-the-art review on manufacturing, topological design, mechanical properties and biocompatibility, *Mater. Sci. Eng., C*, 2017, **76**, 1328–1343, DOI: 10.1016/j.msec.2017.02.094.
- 14 N. M. Rezaei, *et al.*, Biological and osseointegration capabilities of hierarchically (meso-/micro-/nano-scale) roughened zirconia, *Int. J. Nanomed.*, 2018, **13**, 3381–3395, DOI: 10.2147/IJN.S159955.
- 15 N. Shayesteh Moghaddam, *et al.*, Metals for bone implants: safety, design, and efficacy, *Biomanuf. Rev.*, 2016, **1**(1), DOI: 10.1007/s40898-016-0001-2.
- 16 A. Kocijan, *et al.*, Comparative study of superhydrophilic and superhydrophobic TiO<sub>2</sub>/epoxy coatings on AISI 316L stainless steel: surface properties and biocompatibility, *Mater. Technol.*, 2018, **52**(3), 355–361, DOI: 10.17222/mit.2017.190.
- 17 A. Mahato, *et al.*, Applications of Different Bioactive Glass and Glass-Ceramic Materials for Osteoconductivity and Osteoinductivity, *Trans. Indian Ceram. Soc.*, 2017, **76**(3), 149–158, DOI: 10.1080/0371750X.2017.1360799.
- 18 P. Kubasiewicz-Ross, *et al.*, New nano-hydroxyapatite in bone defect regeneration: a histological study in rats, *Ann. Anat.*, 2017, **213**, 83–90, DOI: 10.1016/j.aanat.2017.05.010.
- 19 H. X. Xie, *et al.*, Application of K/Sr co-doped calcium polyphosphate bioceramic as scaffolds for bone substitutes, *J. Mater. Sci.: Mater. Med.*, 2012, **23**(4), 1033–1044, DOI: 10.1007/s10856-012-4556-z.
- 20 A. Kinaci, V. Neuhaus and D. C. Ring, Trends in Bone Graft Use in the United States, *Orthopedics*, 2014, **37**(9), 783–788, DOI: 10.3928/01477447-20140825-54.

- 21 H. Ghanbari and R. Vakili-Ghartavol, Bone Regeneration: Current Status and Future Prospects, in *Advanced Techniques in Bone Regeneration*, A. R. Zorzi and J. B. de Miranda, 2016, IntechOpen, DOI: 10.5772/63912.
- 22 Y. Okazaki and E. Gotoh, Metal release from stainless steel, Co–Cr–Mo–Ni–Fe and Ni–Ti alloys in vascular implants, *Corros. Sci.*, 2008, **50**(12), 3429–3438, DOI: 10.1016/j.corsci.2008.09.002.
- 23 A. Kanaji, *et al.*, Cytotoxic effects of cobalt and nickel ions on osteocytes in vitro, *J. Orthop. Surg. Res.*, 2014, **9**(1), 91, DOI: 10.1186/s13018-014-0091-6.
- 24 J. Zhao, *et al.*, Biodegradation performance of a chitosan coated magnesium-zinc-tricalcium phosphate composite as an implant, *Biointerphases*, 2014, **9**(3), 031004, DOI: 10.1116/1.4881295.
- 25 R. Huiskes, *et al.*, Effects of mechanical forces on maintenance and adaptation of form in trabecular bone, *Nature*, 2000, **405**(6787), 704–706, DOI: 10.1038/35015116.
- 26 C. Boyle and I. Y. Kim, Comparison of different hip prosthesis shapes considering micro-level bone remodeling and stress-shielding criteria using three-dimensional design space topology optimization, *J. Biomech.*, 2011, **44**(9), 1722–1728, DOI: 10.1016/j.jbiomech.2011.03.038.
- 27 S. Bose, D. Banerjee and A. Bandyopadhyay, Introduction to biomaterials and devices for bone disorders, in *Materials and Devices for Bone Disorders*, ed. B. A. Bose S., Academic Press, London, 2016..
- 28 C. T. Wu, *et al.*, Improvement of mechanical and biological properties of porous CaSiO<sub>3</sub> scaffolds by poly(D,L-lactic acid) modification, *Acta Biomater.*, 2008, **4**(2), 343–353, DOI: 10.1016/j.actbio.2007.08.010.
- 29 S. L. Wu, *et al.*, Biomimetic porous scaffolds for bone tissue engineering, *Mater. Sci. Eng., R*, 2014, **80**(1), 1–36, DOI: 10.1016/j.mser.2014.04.001.
- 30 K. Rezwan, Q. Z. Chen and J. J. Blacker, Biodegradable and bioactive porous polymer/inorganic composite scaffolds for bone tissue engineering, *Biomaterials*, 2006, **27**(18), 3413–3431, DOI: 10.1016/j.biomaterials.2006.01.039.
- 31 A. Piroso, *et al.*, Engineering in-vitro stem cell-based vascularized bone models for drug screening and predictive toxicology, *Stem Cell Res. Ther.*, 2018, **9**(1), 112, DOI: 10.1186/s13287-018-0847-8.
- 32 B. L. Seal, T. C. Otero and A. Panitch, Polymeric biomaterials for tissue and organ regeneration, *Mater. Sci. Eng., R*, 2001, **34**(4–5), 147–230, DOI: 10.1016/S0927-796X(01)00035-3.
- 33 H. Jazayeri, *et al.*, The cross-disciplinary emergence of 3D printed bioceramic scaffolds in orthopedic bioengineering, *Ceram. Int.*, 2018, **44**(1), 1–9, DOI: 10.1016/j.ceramint.2017.09.095.
- 34 C. Gao, *et al.*, Bone biomaterials and interactions with stem cells, *Bone Res.*, 2017, **5**, 17059, DOI: 10.1038/boneres.2017.59.
- 35 Y. Xu and J. Guan, Interaction of cells with polyurethane scaffolds, *Advances in Polyurethane Biomaterials*, 2016, pp. 523–542. DOI: 10.1016/B978-0-08-100614-6.00018-4.
- 36 S. Saska, *et al.*, Nanocellulose-collagen-apatite composite associated with osteogenic growth peptide for bone regeneration, *Int. J. Biol. Macromol.*, 2017, **103**, 467–476, DOI: 10.1016/j.ijbiomac.2017.05.086.
- 37 X. Ren, *et al.*, Nanoparticulate mineralized collagen scaffolds induce in vivo bone regeneration independent of progenitor cell loading or exogenous growth factor stimulation, *Biomaterials*, 2016, **89**, 67–78, DOI: 10.1016/j.biomaterials.2016.02.020.
- 38 Z. Zhang, *et al.*, Dehydrothermally crosslinked collagen/hydroxyapatite composite for enhanced in vivo bone repair, *Colloids Surf., B*, 2018, **163**, 394–401, DOI: 10.1016/j.colsurfb.2018.01.011.
- 39 L. Chen, *et al.*, A novel nanocomposite for bone tissue engineering based on chitosan–silk sericin/hydroxyapatite: biomimetic synthesis and its cytocompatibility, *RSC Adv.*, 2015, **5**(69), 56410–56422, DOI: 10.1039/C5RA08216A.
- 40 A. Di Martino, M. Sittlinger and M. V. Risbud, Chitosan: A versatile biopolymer for orthopaedic tissue-engineering, *Biomaterials*, 2005, **26**(30), 5983–5990, DOI: 10.1016/j.biomaterials.2005.03.016.
- 41 M. Stepniewski, J. Martynkiewicz and J. Gosk, Chitosan and its composites: Properties for use in bone substitution, *Polym. Med.*, 2017, **47**(1), 49–53, DOI: 10.17219/pim/76517.
- 42 Y. Lu, *et al.*, High-activity chitosan/nano hydroxyapatite/zoledronic acid (CS/nHA/Zol) scaffolds for simultaneous tumor inhibition, bone repair and infection eradication, *Mater. Sci. Eng., C*, 2018, **82**, 225–233, DOI: 10.1016/j.msec.2017.08.043.
- 43 C. Wu, *et al.*, Mechanically stable surface-hydrophobilized chitosan nanofibrous barrier membranes for guided bone regeneration, *Biomed. Mater.*, 2017, **13**(1), 015004, DOI: 10.1088/1748-605X/aa853c.
- 44 S. Elkholy, *et al.*, In vivo evaluation of  $\beta$ -CS/n-HA with different physical properties as a new bone graft material, *Clin. Implant Dent. Related Res.*, 2018, **20**(3), 416–423, DOI: 10.1111/cid.12599.
- 45 P. Bhattacharjee, *et al.*, Silk scaffolds in bone tissue engineering: An overview, *Acta Biomater.*, 2017, **63**, 1–17, DOI: 10.1016/j.actbio.2017.09.027.
- 46 Silk, Wikipedia, <https://en.wikipedia.org/wiki/Silk>, (accessed December 2018).
- 47 L. Meinel, *et al.*, The inflammatory responses to silk films in vitro and in vivo, *Biomaterials*, 2005, **26**(2), 147–155, DOI: 10.1016/j.biomaterials.2004.02.047.
- 48 L. Lamboni, *et al.*, Silk sericin: A versatile material for tissue engineering and drug delivery, *Biotechnol. Adv.*, 2015, **33**(8), 1855–1867, DOI: 10.1016/j.biotechadv.2015.10.014.
- 49 W. Li, *et al.*, Silk sericin microcapsules with hydroxyapatite shells: protection and modification of organic microcapsules by biomimetic mineralization, *J. Mater. Chem. B*, 2016, **4**(2), 340–347, DOI: 10.1039/C5TB02328A.
- 50 L.-D. Koh, *et al.*, Structures, mechanical properties and applications of silk fibroin materials, *Prog. Polym. Sci.*,

- 2015, **46**, 86–110, DOI: 10.1016/j.procpolymsci.2015.02.001.
- 51 J. Melke, *et al.*, Silk fibroin as biomaterial for bone tissue engineering, *Acta Biomater.*, 2016, **31**, 1–16, DOI: 10.1016/j.actbio.2015.09.005.
  - 52 P. Bhattacharjee, *et al.*, Nanofibrous nonmulberry silk/PVA scaffold for osteoinduction and osseointegration, *Biopolymers*, 2015, **103**(5), 271–284, DOI: 10.1002/bip.22594.
  - 53 K. Ohgo, *et al.*, Preparation of non-woven nanofibers of Bombyx mori silk, Samia cynthia ricini silk and recombinant hybrid silk with electrospinning method, *Polymer*, 2003, **44**(3), 841–846, DOI: 10.1016/S0032-3861(02)00819-4.
  - 54 S. Behera, *et al.*, Hydroxyapatite reinforced inherent RGD containing silk fibroin composite scaffolds: Promising platform for bone tissue engineering, *Nanomedicine*, 2017, **13**(5), 1745–1759, DOI: 10.1016/j.nano.2017.02.016.
  - 55 P. Bhattacharjee, *et al.*, Potential of inherent RGD containing silk fibroin–poly ( $\epsilon$ -caprolactone) nanofibrous matrix for bone tissue engineering, *Cell Tissue Res.*, 2015, **363**(2), 525–540, DOI: 10.1007/s00441-015-2232-6.
  - 56 N. Sahu, *et al.*, Nonmulberry Silk Fibroin Scaffold Shows Superior Osteoconductivity Than Mulberry Silk Fibroin in Calvarial Bone Regeneration, *Adv. Healthcare Mater.*, 2015, **4**(11), 1709–1721, DOI: 10.1002/adhm.201500283.
  - 57 X. Ding, *et al.*, Delivery of demineralized bone matrix powder using a salt-leached silk fibroin carrier for bone regeneration, *J. Mater. Chem. B*, 2015, **3**(16), 3177–3188, DOI: 10.1039/c5tb00046g.
  - 58 H. J. Park, *et al.*, Fabrication of 3D porous SF/ $\beta$ -TCP hybrid scaffolds for bone tissue reconstruction, *J. Biomed. Mater. Res.: Part A*, 2016, **104**(7), 1779–1787, DOI: 10.1002/jbm.a.35711.
  - 59 J. Perez-Rigueiro, *et al.*, Tensile properties of silkworm silk obtained by forced silking, *J. Appl. Polym. Sci.*, 2001, **82**(8), 1928–1935, DOI: 10.1002/app.2038.
  - 60 J. Perez-Rigueiro, *et al.*, Effect of degumming on the tensile properties of silkworm (*Bombyx mori*) silk fiber, *J. Appl. Polym. Sci.*, 2002, **84**(7), 1431–1437, DOI: 10.1002/app.10366.
  - 61 C. Han, *et al.*, Electrophoretic Deposition of Gentamicin-Loaded Silk Fibroin Coatings on 3D-Printed Porous Cobalt–Chromium–Molybdenum Bone Substitutes to Prevent Orthopedic Implant Infections, *Biomacromolecules*, 2017, **18**(11), 3776–3787, DOI: 10.1021/acs.biomac.7b01091.
  - 62 G. Hou, *et al.*, In vivo study of a bioactive nanoparticle-gelatin composite scaffold for bone defect repair in rabbits, *J. Mater. Sci.*, 2017, **28**(11), 181, DOI: 10.1007/s10856-017-5991-7.
  - 63 C. Wang, *et al.*, Bioactive Nanoparticle through Postmodification of Colloidal Silica, *ACS Appl. Mater. Interfaces*, 2014, **6**(7), 4935–4939, DOI: 10.1021/am5014858.
  - 64 D. Gupta, *et al.*, Multiscale porosity in compressible cryogenically 3D printed gel for bone tissue engineering, *ACS Appl. Mater. Interfaces*, 2019, **11**(22), 20437–20452, DOI: 10.1021/acsami.9b05460.
  - 65 Alginic acid, Wikipedia, [https://en.wikipedia.org/wiki/Alginic\\_acid](https://en.wikipedia.org/wiki/Alginic_acid), (accessed December 2018).
  - 66 Alginates, 2015. <https://www.ams.usda.gov/sites/default/files/media/Alginates%20TR%202015.pdf>.
  - 67 J. Venkatesan, *et al.*, Alginate composites for bone tissue engineering: A review, *Int. J. Biol. Macromol.*, 2015, **72**, 269–281, DOI: 10.1016/j.ijbiomac.2014.07.008.
  - 68 M. J. Coathup, *et al.*, The effect of an alginate carrier on bone formation in a hydroxyapatite scaffold, *J. Biomed. Mater. Res. B: Appl. Biomater.*, 2015, **104**(7), 1328–1335, DOI: 10.1002/jbm.b.33395.
  - 69 A. Saltz and U. Kandam, Mesenchymal stem cells and alginate microcarriers for craniofacial bone tissue engineering: A review, *J. Biomed. Mater. Res. Part A*, 2016, **104**(5), 1276–1284, DOI: 10.1002/jbm.a.35647.
  - 70 O. Catanzano, *et al.*, Macroporous alginate foams cross-linked with strontium for bone tissue engineering, *Carbohydr. Polym.*, 2018, 202.
  - 71 S. T. Bendtsen, S. P. Quinnell and M. Wei, Development of a novel alginate-polyvinyl alcohol-hydroxyapatite hydrogel for 3D bioprinting bone tissue engineered scaffolds, *J. Biomed. Mater. Res. Part A*, 2017, **105**(5), 1457–1468, DOI: 10.1002/jbm.a.36036.
  - 72 S. Pacelli, *et al.*, Design of a Cytocompatible Hydrogel Coating to Modulate Properties of Ceramic-Based Scaffolds for Bone Repair, *Cell. Mol. Bioeng.*, 2018, **11**(3), 211–217, DOI: 10.1007/s12195-018-0521-3.
  - 73 R. A. Popescu, *et al.*, New alginate-pullulan-bioactive glass composites with copper oxide for bone tissue regeneration trials, *J. Tissue Eng. Regen. Med.*, 2018, **12**(10), 2112–2121, DOI: 10.1002/term.2746.
  - 74 M. Ataie, I. Shabani and E. Seyedjafari, Surface mineralized Hybrid Nanofibrous Scaffolds Based On Poly(L-lactide) and Alginate Enhances Osteogenic Differentiation of Stem Cells, *J. Biomed. Mater. Res. Part A*, 2019, **107A**, 586–596, DOI: 10.1002/jbm.a.36574.
  - 75 T. I. Shaheen, A. S. Montaser and S. Li, Effect of cellulose nanocrystals on scaffolds comprising chitosan, alginate and hydroxyapatite for bone tissue engineering, *Int. J. Biol. Macromol.*, 2018, **121**, 814–821, DOI: 10.1016/j.ijbiomac.2018.10.081.
  - 76 A. Zheng, *et al.*, Biocompatible silk/calcium silicate/sodium alginate composite scaffolds for bone tissue engineering, *Carbohydr. Polym.*, 2018, **199**, 244–255, DOI: 10.1016/j.carbpol.2018.06.093.
  - 77 J. Leppiniemi, *et al.*, 3D-Printable Bioactivated Nanocellulose–Alginate Hydrogels, *ACS Appl. Mater. Interfaces*, 2017, **9**(26), 21959–21970, DOI: 10.1021/acsami.7b02756.
  - 78 R. Abouzeid, *et al.*, Biomimetic Mineralization of 3D Printed Alginate/TEMPO-Oxidized Cellulose Nanofibril Scaffolds for Bone Tissue Engineering, *Biomacromolecules*, 2018, **19**(11), 4442–4452, DOI: 10.1021/acs.biomac.8b01325.

- 79 S. Tong, *et al.*, In Vitro Culture of BMSCs on VEGF-SF-CS Three-Dimensional Scaffolds for Bone Tissue Engineering, *J. Hard Tissue Biol.*, 2015, **24**(2), 123–133.
- 80 *Biomedical foams for tissue engineering applications*, ed. P. A. Netti, Woodhead Publishing Series in Biomaterials, 2014, vol. 76.
- 81 A. Sionkowska, Current research on the blends of natural and synthetic polymers as new biomaterials: Review, *Prog. Polym. Sci.*, 2011, **36**(9), 1254–1276, DOI: 10.1016/j.progpolymsci.2011.05.003.
- 82 J. Kucinska-Lipka, I. Gubanska and H. Z. Janik, Polyurethanes modified with natural polymers for medical application, *Polymer*, 2014, **59**(3), DOI: 10.14314/polimery.2014.197.
- 83 S. Kashte, A. K. Jaiswal and S. Kadam, Artificial Bone via Bone Tissue Engineering: Current Scenario and Challenges, *J. Tissue Eng. Regen. Med.*, 2017, **14**(1), 1–14, DOI: 10.1007/s13770-016-0001-6.
- 84 C. Ai, *et al.*, Surface modification of vascular endothelial growth factor-loaded silk fibroin to improve biological performance of ultra-high-molecular-weight polyethylene via promoting angiogenesis, *Int. J. Nanomed.*, 2017, **12**, 7737–7750, DOI: 10.2147/IJN.S148845.
- 85 X. Han, *et al.*, Carbon Fiber Reinforced PEEK Composites Based on 3D-Printing Technology for Orthopedic and Dental Applications, *J. Clin. Med.*, 2019, **8**(2), 240, DOI: 10.3390/jcm8020240.
- 86 X. Xu, *et al.*, Triple-functional polyetheretherketone surface with enhanced bacteriostasis and anti-inflammatory and osseointegrative properties for implant application, *Biomaterials*, 2019, **212**, 98–114, DOI: 10.1016/j.biomaterials.2019.05.014.
- 87 E. A. Wakelin, *et al.*, Plasma ion implantation enabled bio-functionalization of PEEK improves osteoblastic activity, *APL Bioeng.*, 2018, **2**(2), 026109, DOI: 10.1063/1.5010346.
- 88 H. Zhu, *et al.*, Tantalum nanoparticles reinforced polyetheretherketone shows enhanced bone formation, *Mater. Sci. Eng. C*, 2019, **101**, 232–242, DOI: 10.1016/j.msec.2019.03.091.
- 89 W. Liu, *et al.*, A surface-engineered polyetheretherketone biomaterial implant with direct and immunoregulatory antibacterial activity against methicillin-resistant *Staphylococcus aureus*, *Biomaterials*, 2019, **208**, 8–20, DOI: 10.1016/j.biomaterials.2019.04.008.
- 90 W. Wang, *et al.*, PEEK surface modification by fast ambient-temperature sulfonation for bone implant applications, *J. R. Soc. Interface*, 2019, **16**(152), 20180955, DOI: 10.1098/rsif.2018.0955.
- 91 J. Khoury, *et al.*, Surface bioactivation of PEEK by neutral atom beam technology, *Bioactive Mater.*, 2019, **4**, 132–141, DOI: 10.1016/j.bioactmat.2019.02.001.
- 92 S. Wang, *et al.*, Strontium/adiponectin co-decoration modulates the osteogenic activity of nano-morphologic polyetheretherketone implant, *Colloids Surf., B*, 2019, **176**, 38–46, DOI: 10.1016/j.colsurfb.2018.12.056.
- 93 B. C. Cheng, *et al.*, Porous titanium-coated polyetheretherketone implants exhibit an improved bone-implant interface: an in vitro and in vivo biochemical, biomechanical, and histological s, *Med. Devices*, 2018, **11**, 391–402.
- 94 X. Yuan, *et al.*, Multifunctional Sulfonated Polyetheretherketone Coating with Beta-defensin-14 for Yielding Durable and Broad-spectrum Antibacterial Activity and Osseointegration, *Acta Biomater.*, 2019, **86**, 323–337, DOI: 10.1016/j.actbio.2019.01.016.
- 95 L. Deng, *et al.*, Dual Therapy Coating on Micro/Nanoscale Porous Polyetheretherketone to Eradicate Biofilms and Accelerate Bone Tissue Repair, *Macromol. Biosci.*, 2018, **19**(2), 1800376, DOI: 10.1002/mabi.201800376.
- 96 S. Mei, *et al.*, Influences of tantalum pentoxide and surface coarsening on surface roughness, hydrophilicity, surface energy, protein adsorption and cell responses to PEEK based biocomposite, *Colloids Surf., B*, 2019, **174**, 207–215, DOI: 10.1016/j.colsurfb.2018.10.081.
- 97 R. Ma and D. Guo, Evaluating the bioactivity of a hydroxyapatite-incorporated polyetheretherketone biocomposite, *J. Orthopaed. Surg. Res.*, 2019, **14**(1), 32, DOI: 10.1186/s13018-019-1069-1.
- 98 R. A. A. Alsaheb, *et al.*, Recent applications of polylactic acid in pharmaceutical and medical industries, *J. Chem. Pharm. Res.*, 2015, **7**(12), 51–63, DOI: 10.2174/1389200218666170919170335.
- 99 A. Larrañaga and J.-R. Sarasua, Poly( $\alpha$ -hydroxy Acids)-Based Cell Microcarriers, *Appl. Sci.*, 2016, **6**(12), 436, DOI: 10.3390/app6120436.
- 100 C.-T. Kao, *et al.*, Poly(dopamine) coating of 3D printed poly(lactic acid) scaffolds for bone tissue engineering, *Mater. Sci. Eng., C*, 2015, **56**, 165–173, DOI: 10.1016/j.msec.2015.06.028.
- 101 V. Guduric, *et al.*, Layer-by-layer bioassembly of cellularized polylactic acid porous membranes for bone tissue engineering, *J. Mater. Sci.: Mater. Med.*, 2017, **28**(5), 78, DOI: 10.1007/s10856-017-5887-6.
- 102 K. Prashantha and F. Roger, Multifunctional properties of 3D printed poly(lactic acid)/graphene nanocomposites by fused deposition modeling, *J. Macromol. Sci., Part A*, 2016, **54**(1), 24–29, DOI: 10.1080/10601325.2017.1250311.
- 103 Q. Chen, *et al.*, 3D Printing Biocompatible Polyurethane/Poly(lactic acid)/Graphene Oxide Nanocomposites: Anisotropic Properties, *ACS Appl. Mater. Interfaces*, 2017, **9**(4), 4015–4023, DOI: 10.1021/acsami.6b11793.
- 104 G. Zhou, *et al.*, Innovative biodegradable poly(L-lactide)/collagen/hydroxyapatite composite fibrous scaffolds promote osteoblastic proliferation and differentiation, *Int. J. Nanomed.*, 2017, **12**, 7577–7588, DOI: 10.2147/IJN.S146679.
- 105 J.-M. Seitz, *et al.*, Recent Advances in Biodegradable Metals for Medical Sutures: A Critical Review, *Adv. Healthcare Mater.*, 2015, **4**(13), 1915–1936, DOI: 10.1002/adhm.201500189.
- 106 K. Van de Velde and P. Kiekens, Biopolymers: overview of several properties and consequences on their applications, *Polym. Test.*, 2002, **21**(4), 433–442.

- 107 S. Petisco-Ferrero, A. Etxeberria and J. R. Sarasua, Mechanical properties and state of miscibility in poly (racD,L-lactide-co-glycolide)/(L-lactide-co-ε-caprolactone) blends, *J. Mech. Behav. Biomed. Mater.*, 2017, **71**, 372–382, DOI: 10.1016/j.jmbbm.2017.04.003.
- 108 X. Wu, *et al.*, Enhanced osteogenic differentiation and bone regeneration of poly(lactic-co-glycolic acid) by graphene via activation of PI3K/Akt/GSK-3β/β-catenin signal circuit, *Biomater. Sci.*, 2018, **6**(5), 1147–1158, DOI: 10.1039/C8BM00127H.
- 109 M. S. Namini, *et al.*, A comparison study on the behavior of human endometrial stem cell-derived osteoblast cells on PLGA/HA nanocomposite scaffolds fabricated by electrospinning and freeze-drying methods, *J. Orthop. Surg. Res.*, 2018, **13**(1), 63, DOI: 10.1186/s13018-018-0754-9.
- 110 K.-S. Park, *et al.*, Versatile effects of magnesium hydroxide nanoparticles in PLGA scaffold-mediated chondrogenesis, *Acta Biomater.*, 2018, **73**, 204–216, DOI: 10.1016/j.actbio.2018.04.022.
- 111 Y. Luo, *et al.*, Enhanced Proliferation and Osteogenic Differentiation of Mesenchymal Stem Cells on Graphene Oxide-Incorporated Electrospun Poly(lactic-co-glycolic acid) Nanofibrous Mats, *ACS Appl. Mater. Interfaces*, 2015, **7**(11), 6331–6339, DOI: 10.1021/acsami.5b00862.
- 112 N. H. Marei, *et al.*, Mesenchymal stem cells growth and proliferation enhancement using PLA vs PCL based nanofibrous scaffolds, *Int. J. Biol. Macromol.*, 2016, **93**(Pt A), 9–19, DOI: 10.1016/j.ijbiomac.2016.08.053.
- 113 Y. Du, *et al.*, Microsphere-based selective laser sintering for building macroporous bone scaffolds with controlled microstructure and excellent biocompatibility, *Colloids Surf., B*, 2015, **135**, 81–89, DOI: 10.1016/j.colsurfb.2015.06.074.
- 114 A. G. B. Castro, *et al.*, Development of a PCL-silica nanoparticles composite membrane for Guided Bone Regeneration, *Mater. Sci. Eng., C*, 2018, **85**, 154–161, DOI: 10.1016/j.msec.2017.12.023.
- 115 W. J. Hendrikson, *et al.*, Influence of PCL molecular weight on mesenchymal stromal cell differentiation, *RSC Adv.*, 2015, **5**(67), 54510–54516, DOI: 10.1039/c5ra08048g.
- 116 E. M. Goncalves, *et al.*, Three-dimensional printed PCL-hydroxyapatite scaffolds filled with CNTs for bone cell growth stimulation, *J. Biomed. Mater. Res. B: Appl. Biomater.*, 2015, **104**(6), 1210–1219, DOI: 10.1002/jbm.b.33432.
- 117 Z. Wang, *et al.*, Osteogenic Potential of Electrospun Poly(3-hydroxybutyrate-co-4-hydroxybutyrate)/Poly(ethylene glycol) Nanofiber Membranes, *J. Biomed. Nanotechnol.*, 2019, **15**(6), 1280–1289, DOI: 10.1166/jbn.2019.2757.
- 118 G. Yang and Z. Cai, Preparation and Characterization of Electrospun Poly(3-Hydroxybutyrate-Co-4-Hydroxybutyrate) Nanofiber Menbranes, *Adv. Mater. Res.*, 2011, **332–334**, 1527–1530, DOI: 10.4028/www.scientific.net/amr.332-334.1527.
- 119 Y. Wu, *et al.*, Preparation, Characterization and In Vitro Biological Evaluation of a Novel Pearl Powder/Poly-Amino Acid Composite as a Potential Substitute for Bone Repair and Reconstruction, *Polymers*, 2019, **11**(5), 831, DOI: 10.3390/polym11050831.
- 120 Q. Fu, *et al.*, Bioactive glass scaffolds for bone tissue engineering: state of the art and future perspectives, *Mater. Sci. Eng., C*, 2011, **31**(7), 1245–1256, DOI: 10.1016/j.msec.2011.04.022.
- 121 A. A. White and S. M. Best, Hydroxyapatite-Carbon Nanotube Composites for Biomedical Applications: A Review, *Int. J. Appl. Ceram. Technol.*, 2007, **4**(1), 1–13, DOI: 10.1111/j.1744-7402.2007.02113.x.
- 122 Q. W. Huang, L. P. Wang and J. Y. Wang, Mechanical properties of artificial materials for bone repair, *J. Shanghai Jiaotong Univ. (Sci)*, 2014, **19**(6), 657–680, DOI: 10.1007/s12204-014-1565-8.
- 123 X. Tian, *et al.*, Recycling and remanufacturing of 3D printed continuous carbon fiber reinforced PLA composites, *J. Cleaner Prod.*, 2017, **142**, 1609–1618, DOI: 10.1016/j.jclepro.2016.11.139.
- 124 N. Xu, *et al.*, 3D Artificial Bones for Bone Repair Prepared by Computed Tomography-Guided Fused Deposition Modeling for Bone Repair, *ACS Appl. Mater. Interfaces*, 2014, **6**(17), 14952–14963, DOI: 10.1021/am502716t.
- 125 A. M. Abdullah, *et al.*, Enhancement of thermal, mechanical and physical properties of polyamide 12 composites via hybridization of ceramics for bone replacement, *Mater. Sci. Eng., C*, 2019, **99**, 719–725, DOI: 10.1016/j.msec.2019.02.007.
- 126 M. Ramu, *et al.*, Optimization of the configuration of porous bone scaffolds made of polyamide/hydroxyapatite composites using selective laser sintering for tissue engineering applications, *Biomed. Mater. Eng.*, 2018, **1**, 1–17, DOI: 10.3233/BME-181020.
- 127 C. Petit, *et al.*, Novel calcium phosphate/PCL graded samples: Design and development in view of biomedical applications, *Mater. Sci. Eng. C: Mater. Biol. Appl.*, 2019, **97**, 336–346, DOI: 10.1016/j.msec.2018.12.044.
- 128 T. Le, *et al.*, Enhancing bioactive properties of silk fibroin with diatom particles for bone tissue engineering applications, *J. Tissue Eng. Regen. Med.*, 2018, **12**(1), 89–97, DOI: 10.1002/term.2373.
- 129 B. Zhang, *et al.*, Tissue-engineered composite scaffold of poly(lactide-co-glycolide) and hydroxyapatite nanoparticles seeded with autologous mesenchymal stem cells for bone regeneration, *J. Zhejiang Univ., Sci., B*, 2017, **18**(11), 963–976, DOI: 10.1631/jzus.B1600412.
- 130 H. Ye, *et al.*, Polyester elastomers for soft tissue engineering, *Chem. Soc. Rev.*, 2018, **47**(12), 4545–4580, DOI: 10.1039/c8cs00161h.
- 131 B. Zylinska, *et al.*, Osteochondral Repair Using Porous Three-dimensional Nanocomposite Scaffolds in a Rabbit Model, *In Vivo*, 2017, **31**(5), 895–903, DOI: 10.21873/in vivo.11144.
- 132 A. Brown, *et al.*, Porous magnesium/PLGA composite scaffolds for enhanced bone regeneration following tooth extraction, *Acta Biomater.*, 2015, **11**, 543–553, DOI: 10.1016/j.actbio.2014.09.008.

- 133 M. Z. Moghadam, *et al.*, Formation of porous HPCL/LPCL/HA scaffolds with supercritical CO<sub>2</sub> gas foaming method, *J. Mech. Behav. Biomed. Mater.*, 2017, **69**, 115–127, DOI: 10.1016/j.jmbbm.2016.12.014.
- 134 J. Guo, *et al.*, Novel porous poly(propylene fumarate-caprolactone) scaffolds fabricated by thermally induced phase separation, *J. Biomed. Mater. Res., Part A*, 2017, **105**(1), 226–235, DOI: 10.1002/jbm.a.35862.
- 135 A. Di Luca, *et al.*, Tailorable Surface Morphology of 3D Scaffolds by Combining Additive Manufacturing with Thermally Induced Phase Separation, *Macromol. Rapid Commun.*, 2017, **38**(16), 1700186, DOI: 10.1002/marc.201700186.
- 136 E. Torino, *et al.*, Synthesis of semicrystalline nanocapsular structures obtained by Thermally Induced Phase Separation in nanoconfinement, *Sci. Rep.*, 2016, **6**, 32727, DOI: 10.1038/srep32727.
- 137 S. Chen and C. Du, Preparation and osteogenic properties of poly (L-lactic acid)/lecithin porous scaffolds with open pore structure, *Zhongguo Xiu Fu Chong Jian Wai Ke Za Zhi*, 2018, **32**(9), 1123–1130, DOI: 10.7507/1002-1892.201804127.
- 138 V. Raeisdasteh Hokmabad, S. Davaran and A. Ramazani, Design and fabrication of porous biodegradable scaffolds: a strategy for tissue engineering, *J. Biomater. Sci., Polym. Ed.*, 2017, **28**(16), 1797–1825, DOI: 10.1080/09205063.2017.1354674.
- 139 K. Shikinaka, K. Shikinaka, Y. Funatsu, Y. Kubota, Y. Tominaga, M. Nakamura, R. R. Navarro, Y. Otsuka, *et al.* Tuneable Shape-Memory Property of Composite based on Nanoparticulated Plant Biomass, Lignin, and Poly(ethylene carbonate), *Soft Matter*, 2018, **14**, 9227–9231, DOI: 10.1039/c8.
- 140 L. P. de Melo, *et al.*, Effect of Injection Molding Melt Temperatures on PLGA Craniofacial Plate Properties during In Vitro Degradation, *Int. J. Biomater.*, 2017, 1–11, DOI: 10.1155/2017/1256537.
- 141 Z. Zhu, *et al.*, Morphology, Thermal, Mechanical Properties and Rheological Behavior of Biodegradable Poly(butylene succinate)/poly(lactic acid) *In situ* Submicrofibrillar Composites, *Materials*, 2018, **11**(12), 2422, DOI: 10.3390/ma11122422.
- 142 T. Zheng, *et al.*, PHBV-graft-GMA via reactive extrusion and its use in PHBV/nanocellulose crystal composites, *Carbohydr. Polym.*, 2018, **205**, 27–34, DOI: 10.1016/j.carbpol.2018.10.014.
- 143 L. Quiles-Carillo, *et al.*, Ductility and Toughness Improvement of Injection-Molded Compostable Pieces of Polylactide by Melt Blending with Poly( $\epsilon$ -caprolactone) and Thermoplastic Starch, *Materials*, 2018, **11**(11), 2138, DOI: 10.3390/ma11112138.
- 144 A. F. Hanafy, *et al.*, Dual effect biodegradable ciprofloxacin loaded implantable matrices for osteomyelitis: controlled release and osteointegration, *Drug Dev. Ind. Pharm.*, 2018, **44**(6), 1023–1033, DOI: 10.1080/03639045.2018.1430820.
- 145 N. Thuaksuban, *et al.*, In vivo biocompatibility and degradation of novel Polycaprolactone-Biphasic Calcium phosphate scaffolds used as a bone substitute, *Biomed. Mater. Eng.*, 2018, **29**(2), 253–267, DOI: 10.3233/BME-171727.
- 146 L. Guo, *et al.*, Enhanced antitumor efficacy of poly(D,L-lactide-co-glycolide)-based methotrexate-loaded implants on sarcoma 180 tumor-bearing mice, *Drug Design, Devel. Ther.*, 2017, **11**, 3065–3075, DOI: 10.2147/DDDT.S143942.
- 147 D. C. De Souza, *et al.*, A fast degrading PLLA composite with a high content of functionalized octacalcium phosphate mineral phase induces stem cells differentiation, *J. Mech. Behav. Biomed. Mater.*, 2019, **93**, 93–104, DOI: 10.1016/j.jmbbm.2019.02.003.
- 148 Y. Zhu, *et al.*, NAC-loaded electrospun scaffolding system with dual compartments for the osteogenesis of rBMSCs in vitro, *Int. J. Nanomed.*, 2019, **14**, 787–798, DOI: 10.2147/IJN.S183233.
- 149 E. Saburi, *et al.*, In vitro osteogenic differentiation potential of the human induced pluripotent stem cells augment when grown on graphene oxide-modified nanofibers, *Gene*, 2019, 72–79, DOI: 10.1016/j.gene.2019.02.028.
- 150 B. Ramesh, K. M. Cherian and A. O. J. Fakoya, Fabrication and Electrospinning of 3D Biodegradable Poly-L-Lactic Acid (PLLA) Nanofibers for Clinical Application, in *Methods in Molecular Biology*, Humana Press, 2019, DOI: 10.1007/7651\_2019\_213.
- 151 Z. Bazrafshan and G. K. Stylios, Spinnability of collagen as a biomimetic material: A review, *Int. J. Biol. Macromol.*, 2019, **129**, 693–705, DOI: 10.1016/j.ijbiomac.2019.02.024.
- 152 T. T. Demirtaş, G. Irmak and M. Gümüşderelioğlu, A bio-printable form of chitosan hydrogel for bone tissue engineering, *Biofabrication*, 2017, **9**(3), DOI: 10.1088/1758-5090/aa7b1d.
- 153 P. Lohmann, *et al.*, Bone regeneration induced by a 3D architected hydrogel in a rat critical-size calvarial defect, *Biomaterials*, 2017, **113**, 158–169, DOI: 10.1016/j.biomaterials.2016.10.039.
- 154 S. M. Hamlet, *et al.*, 3-Dimensional functionalized polycaprolactone-hyaluronic acid hydrogel constructs for bone tissue engineering, *J. Clin. Periodontol.*, 2017, **44**(4), 428–437, DOI: 10.1111/jcpe.12686.
- 155 A. H. Aziz, *et al.*, The effects of dynamic compressive loading on human mesenchymal stem cell osteogenesis in the stiff layer of a bilayer hydrogel, *J. Tissue Eng. Regener. Med.*, 2019, **13**(6), 946–959, DOI: 10.1002/term.2827.
- 156 M. Kurian, R. Stevens and K. McGrath, Towards the Development of Artificial Bone Grafts: Combining Synthetic Biomineralisation with 3D Printing, *J. Funct. Biomater.*, 2019, **11**(1), 12, DOI: 10.3390/jfb10010012.
- 157 O. Catanzano, *et al.*, Macroporous alginate foams cross-linked with strontium for bone tissue engineering, *Carbohydr. Polym.*, 2018, **202**, 72–83, DOI: 10.1016/j.carbpol.2018.08.086.
- 158 E. Saloni, *et al.*, Gas-foamed poly(lactide-co-glycolide) and poly(lactide-co-glycolide) with bioactive glass fibres demonstrate insufficient bone repair in lapine osteochondral defects, *J. Tissue Eng. Regener. Med.*, 2019, **13**(3), 406–415, DOI: 10.1002/term.2801.

- 159 X. Jing, H.-Y. Mi and L.-S. Turng, Comparison between PCL/hydroxyapatite (HA) and PCL/halloysite nanotube (HNT) composite scaffolds prepared by co-extrusion and gas foaming, *Mater. Sci. Eng., C*, 2017, **72**, 53–61, DOI: 10.1016/j.msec.2016.11.049.
- 160 A. Wubneh, *et al.*, Current State of Fabrication Technologies and Materials for Bone Tissue Engineering, *Acta Biomater.*, 2018, **80**, 1–30, DOI: 10.1016/j.actbio.2018.09.031.
- 161 Y. Li, *et al.*, Adaptive Structured Pickering Emulsions and Porous Materials Based on Cellulose Nanocrystal Surfactants, *Angew. Chem., Int. Ed.*, 2018, **57**(41), 13560–13564, DOI: 10.1002/anie.201808888.
- 162 A. R. V. Morais, *et al.*, Freeze-drying of emulsified systems: A review, *Int. J. Pharm.*, 2016, **503**(1–2), 102–114, DOI: 10.1016/j.ijpharm.2016.02.047.
- 163 A. Bandyopadhyay, S. Bose and S. Das, 3D printing of biomaterials, *MRS Bull.*, 2015, **40**(02), 108–115, DOI: 10.1557/mrs.2015.3.
- 164 Y. Xu, *et al.*, Construction of bionic tissue engineering cartilage scaffold based on three-dimensional printing and oriented frozen technology, *J. Biomed. Mater. Res., Part A*, 2018, **106**(6), 1664–1676, DOI: 10.1002/jbm.a.36368.
- 165 A. Yahamed, *et al.*, Mechanical properties of 3D printed polymers, *J. Print Media Technol. Res.*, 2016, **5**, 273–289, DOI: 10.14622/JPMTR-1608.
- 166 D. K. Mills, *et al.*, Studies on the cytocompatibility, mechanical and antimicrobial properties of 3D printed poly(methyl methacrylate) beads, *Bioact. Mater.*, 2018, **3**(2), 157–166, DOI: 10.1016/j.bioactmat.2018.01.006.
- 167 Z. Dai, *et al.*, Biomimetic hydroxyapatite/poly xylitol sebacic adipate/vitamin K nanocomposite for enhancing bone regeneration, *Artif. Cells, Nanomed., Biotechnol.*, 2019, **47**(1), 1898–1907, DOI: 10.1080/21691401.2019.1573183.
- 168 W. Zhao, *et al.*, D-RADA16-RGD-Reinforced Nano-Hydroxyapatite/Polyamide 66 Ternary Biomaterial for Bone Formation, *Tissue Eng. Regen. Med.*, 2019, **16**(2), 177–189, DOI: 10.1007/s13770-018-0171-5.
- 169 Y. Zhang, *et al.*, Adhesion and Proliferation of Osteoblast-Like Cells on Porous Polyetherimide Scaffolds, *BioMed Res. Int.*, 2018, **2018**, 1491028, DOI: 10.1155/2018/1491028.
- 170 M. Ziabka, M. Dziadek and E. Menaszek, Biocompatibility of Poly(acrylonitrile-butadiene-styrene) Nanocomposites Modified with Silver Nanoparticles, *Polymers*, 2018, **10**(11), 1257, DOI: 10.3390/polym10111257.
- 171 Y. Wang, *et al.*, Optimized Synthesis of Biodegradable Elastomer PEGylated Poly(glycerol sebacate) and Their Biomedical Application, *Polymers*, 2019, **11**(6), 965, DOI: 10.3390/polym11060965.
- 172 A. Tevlek, *et al.*, Bi-layered constructs of poly(glycerol-sebacate)- $\beta$ -tricalcium phosphate for bone-soft tissue interface applications, *Mater. Sci. Eng., C*, 2017, **72**, 316–324, DOI: 10.1016/j.msec.2016.11.082.
- 173 S. Salehi, *et al.*, Poly (glycerol sebacate)-poly ( $\epsilon$ -caprolactone) blend nanofibrous scaffold as intrinsic bio- and immunocompatible system for corneal repair, *Acta Biomater.*, 2017, **50**, 370–380, DOI: 10.1016/j.actbio.2017.01.013.
- 174 S. Chung and T. J. Webster, Antimicrobial nanostructured polyurethane scaffolds, *Adv. Polyurethane Biomater.*, 2016, 503–521, DOI: 10.1016/B978-0-08-100614-6.00017-2.
- 175 I. Chiulan, *et al.*, Recent Advances in 3D Printing of Aliphatic Polyesters, *Bioengineering*, 2017, **5**(1), 2, DOI: 10.3390/bioengineering5010002.
- 176 C. Murphy, *et al.*, 3D bioprinting of stem cells and polymer/bioactive glass composite scaffolds for bone tissue engineering, *Int. J. Bioprint.*, 2017, **3**(1), 54–64, DOI: 10.18063/IJB.2017.01.005.
- 177 M. N. Rahaman, *et al.*, Bioactive glass in tissue engineering, *Acta Biomater.*, 2011, **7**(6), 2355–2373, DOI: 10.1016/j.actbio.2011.03.016.
- 178 C. Hull, On Stereolithography, *Virtual Phys. Prototyping*, 2012, **7**(3), 177, DOI: 10.1080/17452759.2012.723409.
- 179 J. L. Walker and M. Santoro, Processing and production of bioresorbable polymer scaffolds for tissue engineering, in *Bioresorbable Polymers for Biomedical Applications*. 2017, Woodhead Publishing, pp. 181–203. DOI: 10.1016/B978-0-08-100262-9.00009-4.
- 180 A visual Ultimaker Troubleshooting guide, 3DVerkstan, 2017, <https://support.3dverkstan.se/article/23-a-visual-ultimaker-troubleshooting-guide#nostick>, (accessed March 2019).
- 181 A. Jennings, 3D Printing Troubleshooting 41 Common Problems in 2019, 2019, <https://all3dp.com/1/common-3d-printing-problems-troubleshooting-3d-printer-issues/>, (accessed March 2019).
- 182 Post-Process Your SLA Prints in 4 Easy Steps, Kudo3D, <https://www.kudo3d.com/post-process-your-sla-prints-in-4-easy-steps/>, (accessed March 2019).
- 183 K. Salonitis, Stereolithography, *Compr. Mater. Process.*, 2014, **10**, 19–67, DOI: 10.1016/B978-0-08-096532-1.01001-3.
- 184 M. Vaezi and S. Yang, Freeform fabrication of nanobiomaterials using 3D printing, in *Rapid Prototyping of Biomaterials*. 2014, Woodhead Publishing, pp. 16–74. DOI: 10.1533/9780857097217.16.
- 185 C.-S. Wu and H.-T. Liao, Fabrication, characterization, and application of polyester/wood flour composites, *J. Polym. Eng.*, 2017, **37**(7), 689–698, DOI: 10.1515/polyeng-2016-0284.
- 186 C.-S. Wu, H.-T. Liao and Y.-X. Cai, Characterisation, biodegradability and application of palm fibre-reinforced polyhydroxyalkanoate composites, *Polym. Degrad. Stab.*, 2017, **140**, 55–63, DOI: 10.1016/j.polymdegradstab.2017.04.016.
- 187 D. Filgueira, *et al.*, Enzymatic-Assisted Modification of Thermomechanical Pulp Fibers To Improve the Interfacial Adhesion with Poly(lactic acid) for 3D Printing, *ACS Sustainable Chem. Eng.*, 2017, **5**(10), 9338–9346, DOI: 10.1021/acssuschemeng.7b02351.
- 188 M. C. Wurm, *et al.*, In-vitro evaluation of Polylactic acid (PLA) manufactured by fused deposition modeling, *J. Biol. Eng.*, 2017, **11**(1), 29, DOI: 10.1186/s13036-017-0073-4.
- 189 V. C. Mow and R. Huiskes, *Basic Orthopaedic Biomechanics and Mechano-Biology*, Lippincott Williams & Wilkins, Philadelphia, 3rd edn, 2005.

- 190 O. I. Parisi, M. Curcio and F. Puoci, Polymer Chemistry and Synthetic Polymers, in *Advanced Polymers in Medicine*, ed. F. Puoci, 2015, pp. 1–31, DOI: 10.1007/978-3-319-12478-0.
- 191 Y. Hong, Electrospun fibrous polyurethane scaffolds in tissue engineering, *Adv. Polyurethane Biomater.*, 2016, 543–559, DOI: 10.1016/B978-0-08-100614-6.00019-6.
- 192 R. Guo, *et al.*, Fabrication of 3D Scaffolds with Precisely Controlled Substrate Modulus and Pore Size by Templated-Fused Deposition Modeling to Direct Osteogenic Differentiation, *Adv. Healthcare Mater.*, 2015, 4(12), 1826–1832, DOI: 10.1002/adhm.201500099.
- 193 W. C. Oliver and G. M. Pharr, An improved technique for determining hardness and elastic modulus using load and displacement sensing indentation experiments, *J. Mater. Res.*, 1992, 7(6), 1564–1583, DOI: 10.1557/JMR.1992.1564.
- 194 K. E. Smith, *et al.*, The dependence of MG63 osteoblast responses to (meth)acrylate-based networks on chemical structure and stiffness, *Biomaterials*, 2010, 31(24), 6131–6141, DOI: 10.1016/j.biomaterials.2010.04.033.
- 195 K. J. Tsai, *et al.*, Biomimetic heterogenous elastic tissue development, *npj Regener. Med.*, 2017, 2(1), 16, DOI: 10.1038/s41536-017-0021-4.
- 196 K. Lehle, *et al.*, In vitro Endothelialization and Platelet Adhesion on Titaniferous Upgraded Polyether and Polycarbonate Polyurethanes, *Materials*, 2014, 7(2), 623–636, DOI: 10.3390/ma7020623.
- 197 W. Zhao, *et al.*, Shape memory polymers and their composites in biomedical applications, *Mater. Sci. Eng., C*, 2018, 97, 864–883, DOI: 10.1016/j.msec.2018.12.054.
- 198 T. Liu, *et al.*, Stimulus methods of multi-functional shape memory polymer nanocomposites: A review, *Composites, Part A*, 2017, 100, 20–30, DOI: 10.1016/j.compositesa.2017.04.022.
- 199 Y. Okazaki and E. Gotoh, Metal release from stainless steel, Co-Cr-Mo-Ni-Fe and Ni-Ti alloys in vascular implants, *Corros. Sci.*, 2008, 50, 3429–3438, DOI: 10.1016/j.corsci.2008.09.002.
- 200 J. Sevcikova and M. Pavkova Goldbergova, Biocompatibility of NiTi alloys in the cell behaviour, *Biometals*, 2017, 30(2), 163–169, DOI: 10.1007/s10534-017-0002-5.
- 201 A. Mirhashemi, S. Jahangiri and M. J. Kharrazifard, Release of nickel and chromium ions from orthodontic wires following the use of teeth whitening mouthwashes, *Prog. Orthod.*, 2018, 19(1), 4, DOI: 10.1186/s40510-018-0203-7.
- 202 R. Hang, *et al.*, Length-dependent corrosion behavior, Ni<sup>2+</sup> release, cytocompatibility, and antibacterial ability of Ni-Ti-O nanopores anodically grown on biomedical NiTi alloy, *Mater. Sci. Eng., C*, 2018, 89, 1–7, DOI: 10.1016/j.msec.2018.03.018.
- 203 S. Latvala, *et al.*, Nickel Release, ROS Generation and Toxicity of Ni and NiO Micro- and Nanoparticles, *PLoS One*, 2016, 11(7), e0159684, DOI: 10.1371/journal.pone.0159684.
- 204 G. Du, *et al.*, Nacre-mimetic composite with intrinsic self-healing and shape-programming capability, *Nat. Commun.*, 2019, 10(1), 800, DOI: 10.1038/s41467-019-08643-x.
- 205 T. Li, *et al.*, Thermally and Near-Infrared Light-Induced Shape Memory Polymers Capable of Healing Mechanical Damage and Fatigued Shape Memory Function, *ACS Appl. Mater. Interfaces*, 2019, 11(9), 9470–9477, DOI: 10.1021/acsami.8b21970.
- 206 F. S. L. Bobbert, J. Janbaz and A. A. Zadpoor, Towards deployable meta-implants, *J. Mater. Chem. B*, 2018, 6, 3449–3455, DOI: 10.1039/C8TB00576A.
- 207 A. A. Zadpoor, Deployable meta-implants, 2018, <https://www.youtube.com/watch?v=MDklBod0yUM>, (accessed March 2019).
- 208 A. Arnebold and A. Hartwig, Fast switchable epoxy based shape-memory polymers with high strength and toughness, *Polymer*, 2016, 83, 40–49, DOI: 10.1016/j.polymer.2015.12.007.
- 209 M. Gupta, *et al.*, Programmable Mechanical Properties from a Worm Jaw-derived Biopolymer through Hierarchical Ion Exposure, *ACS Appl. Mater. Interfaces*, 2018, 10(38), 31928–31937, DOI: 10.1021/acsami.8b10107.
- 210 J. B. Costa, *et al.*, Fast Setting Silk Fibroin Bioink for Bioprinting of Patient-Specific Memory-Shape Implants, *Adv. Healthcare Mater.*, 2017, 6(22), 1701021, DOI: 10.1002/adhm.201701021.
- 211 N. Li, *et al.*, Multivalent cations-triggered rapid shape memory sodium carboxymethyl cellulose/polyacrylamide hydrogels with tunable mechanical strength, *Carbohydr. Polym.*, 2017, 178, 159–165, DOI: 10.1016/j.carbpol.2017.09.030.
- 212 Y. Zhang, *et al.*, Bio-inspired layered chitosan/graphene oxide nanocomposite hydrogels with high strength and pH-driven shape memory effect, *Carbohydr. Polym.*, 2017, 177, 116–125, DOI: 10.1016/j.carbpol.2017.08.106.
- 213 J. Ban, *et al.*, The Effect of 4-Octyldecyloxybenzoic Acid on Liquid-Crystalline Polyurethane Composites with Triple-Shape Memory and Self-Healing Properties, *Materials*, 2016, 9(9), 792, DOI: 10.3390/ma9090792.
- 214 W. J. Hendrikson, *et al.*, Towards 4D printed scaffolds for tissue engineering: exploiting 3D shape memory polymers to deliver time-controlled stimulus on cultured cells, *Biofabrication*, 2017, 9(3), 031001, DOI: 10.1088/1758-5090/aa8114.
- 215 Z. Deng, *et al.*, Stretchable degradable and electroactive shape memory copolymers with tunable recovery temperature enhance myogenic differentiation, *Acta Biomater.*, 2016, 46, 234–244, DOI: 10.1016/j.actbio.2016.09.019.
- 216 K. Kawaguchi, *et al.*, Effects of chitosan fiber addition on the properties of polyurethane with thermo-responsive shape memory, *J. Biomed. Mater. Res., Part B*, 2016, 105(5), 1151–1156, DOI: 10.1002/jbm.b.33664.
- 217 L. Tan, *et al.*, Study of multi-functional electrospun composite nanofibrous mats for smart wound healing, *Int. J. Biol. Macromol.*, 2015, 79, 469–476, DOI: 10.1016/j.ijbiomac.2015.05.014.
- 218 R. Ferracini, *et al.*, Scaffolds as Structural Tools for Bone-Targeted Drug Delivery, *Pharmaceutics*, 2018, 10(3), 122, DOI: 10.3390/pharmaceutics10030122.

- 219 K. Ficek, *et al.*, A bioresorbable polylactide implant used in bone cyst filling, *J. Mater. Sci.: Mater. Med.*, 2016, **27**(2), 1–8, DOI: 10.1007/s10856-015-5647-4.
- 220 I. Krucinska, *et al.*, Biological Properties of Low-Toxicity PLGA and PLGA/PHB Fibrous Nanocomposite Implants for Osseous Tissue Regeneration. Part I: Evaluation of Potential Biototoxicity, *Molecules*, 2017, **22**(12), 2092, DOI: 10.3390/molecules22122092.
- 221 O. Hasturk, *et al.*, Square prism micropillars improve osteogenicity of poly(methyl methacrylate) surfaces, *J. Mater. Sci.: Mater. Med.*, 2018, **29**(5), 1, DOI: 10.1007/s10856-018-6059-z.
- 222 A. Di Martino, M. Sittiger and M. V. Risbud, Chitosan: A versatile biopolymer for orthopaedic tissue-engineering, *Biomaterials*, 2005, **26**(30), 5983–5990, DOI: 10.1016/j.biomaterials.2005.03.016.
- 223 A. R. Boccaccini, *et al.*, Polymer/bioactive glass nanocomposites for biomedical applications: A review, *Compos. Sci. Technol.*, 2010, **70**(13), 1764–1776, DOI: 10.1016/j.compscitech.2010.06.002.
- 224 A. Aijaz, *et al.*, Hydrogel microencapsulated insulin-secreting cells increase keratinocyte migration, epidermal thickness, collagen fiber density, and wound closure in a diabetic mouse model of wound healing, *Tissue Eng., Part A*, 2015, **21**(21–22), DOI: 10.1089/ten.TEA.2015.0069.
- 225 G. Yang, *et al.*, Counterionic biopolymers-reinforced bioactive glass scaffolds with improved mechanical properties in wet state, *Mater. Lett.*, 2012, **75**, 80–83, DOI: 10.1016/j.matlet.2012.01.122.
- 226 J. Hadzik, *et al.*, New nano-hydroxyapatite in bone defect regeneration: a histological study in rats, *Ann. Anat.*, 2017, **213**, 83–90.
- 227 C. Gao, *et al.*, Robotic deposition and in vitro characterization of 3D gelatin–bioactive glass hybrid scaffolds for biomedical applications, *J. Biomed. Mater. Res., Part A*, 2013, **101A**(7), 2027–2037, DOI: 10.1002/jbm.a.34496.
- 228 B. Lei, *et al.*, Porous gelatin–siloxane hybrid scaffolds with biomimetic structure and properties for bone tissue regeneration, *J. Biomed. Mater. Res., Part B*, 2014, **102B**, 1528–1536, DOI: 10.1002/jbm.b.33133.